The Origin of Systematic Errors in the GCM Simulation of ITCZ Precipitation over Oceans

Winston C. Chao[1], Max J. Suarez[1], Julio T. Bacmeister[2],

Baode Chen[3] and Lawrence L. Takacs[3]

1 NASA/Goddard Space Flight Center, Greenbelt, MD 20771

2 Goddard Earth Sciences and Technology Center, University of Maryland, Baltimore County, Baltimore, MD 21250

3 Science Applications International Corporation, Lanham, MD 20706

April 2006

Corresponding Author Address:
Dr. Winston C. Chao
Mail Code 613.2
NASA/GSFC
Greenbelt, MD 20771

Winston.c.chao@nasa.gov

Abstract

This study provides explanations for some of the experimental findings of Chao (2000) and Chao and Chen (2001) concerning the mechanisms responsible for the ITCZ in an aqua-planet model. These explanations are then applied to explain the origin of some of the systematic errors in the GCM simulation of ITCZ precipitation over oceans. The ITCZ systematic errors are highly sensitive to model physics and by extension model horizontal resolution. The findings in this study along with those of Chao (2000) and Chao and Chen (2001, 2004) contribute to building a theoretical foundation for ITCZ study. A few possible methods of alleviating the systematic errors in the GCM simulation of ITCZ are discussed. This study uses a recent version of the Goddard Modeling and Assimilation Office's Goddard Earth Observing System (GEOS-5) GCM.

1. Introduction

The latent heat released in the intertropical convergence zone (ITCZ) drives (or, more precisely, interacts with) the Hadley/Walker circulation; thus the realism of the location and intensity of the ITCZ precipitation simulated in a general circulation model (GCM) is a fundamental factor in the performance of a GCM. The ITCZ precipitation in most GCMs has large systematic errors. In some GCMs the ITCZ precipitation in the western and central Pacific in the June-July-August (JJA) season, when the SST peak is in the northern hemisphere, can be so unrealistic as to have a maximum in the southern--the incorrect--hemisphere (e.g., in the NCAR CCM3 as shown in Fig. 22 of Hack et al. 1998, in an earlier version of the NASA seasonal-to-interannual prediction project (NSIPP) model (Fig. 1 of Bacmeister et al. 2006), and in NCAR CCSM3 (Fig. 1a of Zhang and Wang 2006)). Since these models also show a concurrent weaker northern ITCZ in the same regions, there is a distinct "double ITCZ signature." In the Dec-Jan-Feb season a similar wrong hemisphere problem may also exist in the same regions (e.g., Fig. 21 of Hack et al. 1998).

A related issue is why the maximum GCM-simulated ITCZ precipitation does not appear in the wrong hemisphere in the eastern Pacific or the Atlantic in the JJA season. Most GCMs, after some empirical modifications, may not have such an extreme as maximum ITCZ precipitation in the wrong hemisphere, but they still have the lesser problem of wrong ITCZ intensity. Why the empirical modifications helped in removing the wrong hemisphere problem and how the remaining problems can be resolved are

additional questions. Another problem common among the GCMs is the dip in the ITCZ precipitation in the middle of the northeastern Pacific—i.e., the precipitation tends to concentrate in the coastal region next to Central America, where there is a local SST maximum. Such high concentration of ITCZ precipitation over local SST maxima also occurs in equatorial western Atlantic in some models. Moreover, in some models the ITCZ precipitation peak in the Indian Ocean may locate at an equatorial location in the JJA season.

Correcting these ITCZ precipitation systematic errors is an important area of research that has attracted many researchers (e.g., Wu et al. 2003, Bacmeister et al. 2006, and Zhang and Wang 2006). Grasping the origin of these systematic errors would aid in correcting them. The purpose of this paper is to study the origin of these systematic errors in an attempt to contribute to the larger goal of building a theoretical foundation for ITCZ study. The previous theoretical and modeling studies by Chao (2000) and Chao and Chen (2001, 2004) of the ITCZ using an aqua-planet model provide a starting point for this study. Below, we will briefly review these aqua-planet ITCZ studies and apply the knowledge gained there to the problems at hand. We will also support our findings by GCM experiments using a recent version of the Goddard Earth Observing System (GEOS-5) GCM.

2. Brief review of the fundamental mechanisms governing the ITCZ's latitudinal location in aqua-planet settings

To proceed with our study, we need to delve into the fundamental physical mechanisms that are responsible for the ITCZ. These mechanisms are most clearly revealed in aqua-planet (AP) GCM simulations. AP GCMs, with zonally-uniform sea surface temperature (SST), provide simplified settings to examine the ITCZ. Under these settings the latitudinal location of the ITCZ is determined by the earth's rotation, interaction among model physics components, and the SST latitudinal profile. A more basic AP model setting is one without variations in SST and solar angle. This case will be reviewed first. The case of SST varying only in the latitudinal direction will be reviewed subsequently.

2.a *Aqua-planet model with globally-uniform SST and solar angle*

The study of the ITCZ in an AP model with globally- and temporally-uniform SST and solar angle by Chao and Chen (2004) showed that the ITCZ under such settings could be either a single ITCZ over the equator or a double ITCZ at approximately 15N&S depending on the model physics. Sometimes only one component of the double ITCZ appears (this remains a puzzle; others have obtained the same phenomenon with different models (e.g., Raymond 2000)); still a single ITCZ away from the equator is distinctly different from a single ITCZ over the equator. Whether a single or a double ITCZ appears is determined by the earth's rotation, the interaction between convection and surface fluxes through earth's rotation, and the interaction between convection and radiation. Since convection is central to these interactions, the cumulus parameterization scheme plays a very important role in GCM simulation of ITCZ.

Chao and Chen (2001) performed some experiments in which the relaxed Arakawa-Schubert scheme (RAS, Moorthi and Suarez 1992) was allowed to operate only when the boundary layer relative humidity rose above a certain critical value. By increasing this critical value the behavior of the cumulus scheme could be changed from that of RAS to that of the moist convective adjustment scheme (MCA, Manabe et al. 1965), and the ITCZ could be correspondingly changed from a double ITCZ to a single ITCZ over the equator.

Chao and Chen (2004) theorized that under uniform SST and solar angle conditions the ITCZ experiences two opposing types of attraction--both due to the earth's rotation--and that the latitude where these two attractions balance each other is where the ITCZ resides. The first type of attraction is due to inertial stability, which pulls the ITCZ toward the equator (see Section 3 of Chao and Chen (2001) for an explanation). This attraction does not depend on the model physics. The second type of attraction on the ITCZ is due to the latitudinal gradient of the Coriolis parameter-modified surface heat fluxes in association with synoptic convective systems, which pulls the ITCZ toward one of the poles. The degree of modification of surface heat fluxes by the Coriolis parameter depends on the cumulus parameterization scheme, among other components of the model physics.

The magnitudes of these two types of attraction on the ITCZ as functions of latitude are depicted schematically in Fig. 15 of Chao and Chen (2004), which is reproduced here as Fig. 1. The magnitude of the first type of attraction—represented as curve A (a positive value means southward attraction)--is equal to $8\Omega \sin\phi \cos\phi$ with Ω being the earth's rotation rate and ϕ the latitude. The magnitude of the second type of

attraction—represented as curve B (a positive value means northward attraction)--is depicted for RAS and MCA. Chao and Chen (2004) gave the interpretation that the conditions for MCA to operate are more restrictive than that for RAS, and therefore under MCA the modeled synoptic convective systems are more vigorous, and thus the associated surface wind--and in turn, the surface fluxes--are less affected by the earth's rotation. This is because after an air parcel moves down into the boundary layer, it moves quickly towards the center of the convective systems and spends a very short time in being affected by the Coriolis force to increase its speed. As a result, curve Bmca is weaker than Bras. Curve A is derived analytically and curve B is constructed based on both numerical experimental results and theoretical arguments; see Chao and Chen (2004) for details.

For RAS the stable balance between the two types of attraction is at approximately 14N&S and for MCA the stable balance is at the equator. (These locations are called the centers of rotational ITCZ attractors (Chao and Chen 2001)). Therefore, RAS yields a double ITCZ straddling the equator, whereas MCA yields a single ITCZ over the equator. The net attraction on the ITCZ (a positive value means southward attraction) is depicted as curve R in Fig. 2a and Fig. 2b for RAS and MCA, respectively (reproduced from Chao (2000)).

When a condition that the boundary layer relative humidity must be above a certain critical value is added to RAS, the condition for RAS to operate becomes stricter and RAS behaves more like MCA; i.e., in Fig.1, Bras is reduced to Bmca as this critical value increases. As a result a double ITCZ turns into a single ITCZ.

Chao and Chen (2004) pointed out that the failure of earlier ITCZ theories in explaining the ITCZ latitudinal location in AP models with globally –uniform SST and solar angle was due to the failure of CISK and wave-CISK theories and to not recognizing the existence of curve B in Fig. 1.

2.b *Aqua-planet model with an SST latitudinal profile*

When the SST distribution is changed from globally-uniform to latitudinal-varying (but zonally-uniform) and is given a Gaussian-shape latitudinal dependence, the ITCZ experiences an additional type of attraction towards a latitude offset slightly poleward from the SST peak. This is shown in Fig. 11 of Chao (2000), in an experiment without the earth's rotation. In this experiment with the Coriolis parameter f set to zero as the SST peak is moved poleward--and with the shape of the SST latitudinal Gaussian profile unchanged--the ITCZ offset from the SST peak increases[1]. But this offset remains small. This new type of attraction is depicted in Figs. 2a and 2b as line S. Chao (2000) gave an explanation as to why this attraction could be approximately represented by a linear line. Obviously, the slope of line S (or its closeness to a vertical line) is an indication of the strength of the attraction due to the SST peak.

When both the earth's rotation and a Gaussian SST latitudinal profile exist within an experiment, the balance in Fig. 2 of curve R (a positive value means southward

[1] The explanation for the poleward offset of the ITCZ from the SST peak is as follows: When the SST peak is at the equator in this experiment, the equator is the latitude of symmetry and the ITCZ is located there.; but when the SST peak is moved away from the equator, the earth's geometry is no longer symmetric with respect to the SST peak. The poleward side of the SST peak has a higher averaged SST and thus the ITCZ is located slightly poleward of the SST peak. The degree of the asymmetry and thus that of the offset becomes larger as the SST peak is moved farther away from the equator.

attraction)--representing the rotational forcing (i.e., the difference between curves A and B in Fig. 1)--and line S (a positive value means northward attraction) determines the latitudinal location of the ITCZ for both RAS and MCA. If RAS is used and the SST peak remains at the equator and becomes sharper--i.e., line S becomes more vertical--the two components of the double ITCZ draw closer and eventually merge; see Fig. 13 of Chao (2000) for the result of such an experiment.

If the SST Gaussian latitudinal profile retains its shape but is moved latitudinally, the ITCZ structure can change quite substantially. Figs. 11 and 10 of Chao and Chen (2001) show the results of such an experiment for both MCA and RAS types of convection schemes, respectively. When MCA is used and the SST peak is moved northward from the equator, consistent with Fig. 2a, a single ITCZ follows behind the SST peak and then suddenly starts to catch up with the SST peak, but does not quite reach the SST peak, and thereafter the ITCZ appears to be almost stationary despite further northward movement of the SST peak. When RAS is used, there are two balance latitudes if the SST peak is not too far away from the equator (Fig. 2b). Thus, there is a double ITCZ. As the SST peak moves northward from the equator, both ITCZ components move northward and the southern component of the double ITCZ becomes stronger than the northern component. Finally, the southern ITCZ moves rapidly to merge with the northern component, and thereafter the merged single ITCZ remains almost stationary despite further northward movement of the SST peak. This phenomenon, shown in Fig. 3.b of Chao and Chen (2001), has not been previously explained. The explanation for this phenomenon is a prerequisite of our answer to the theoretical questions asked in the introduction and will be given in the next section.

2.c *Remarks*

Our interpretation of the AP experimental results does not have to assume that the rotational attraction and the SST peak attraction on the ITCZ should be linearly added. See the Appendix for a discussion of this additive assumption.

3. Explanation for the systematic errors in ITCZ precipitation

3.a *Explanation for Fig. 3 of Chao and Chen (2001)*

The explanation for the ITCZ behavior illustrated in Fig. 3. of Chao and Chen (2001) is as follows. There is a nearly vertical demarcation line in the zonal mean meridional circulation separating the northern components of the meridional circulation cells from the southern components. One may call the latitude of this demarcation line the "meridional circulation equator (MCE)." When the SST peak is at the equator, the MCE is there too. When the SST peak is moved northward from the equator, the MCE--which lies midway between the two ITCZ components that are moving northward--should move northward as well. As the MCE moves north of the equator, the global area south of the MCE becomes larger than that north of the MCE. Since the southern component of the double ITCZ is now responsible for heating a larger area, it is expected

to become stronger than the northern component of the double ITCZ[2]. Thus, as the SST peak is moved north from the equator, the southern component of the double ITCZ strengthens. As the SST peak is moved further north away from the equator, its attraction no longer balances the two rotational attractors separately. Now, in Fig. 2.b, line S no longer intersects curve R south of the equator--i.e., the attraction due to the SST peak has to deal with the two rotational attractors as a whole. Therefore, the double ITCZ now becomes a single ITCZ—i.e., the southern component of the double ITCZ moves rapidly to merge with the northern one.

3.b *Explanation for how the simulated ITCZ maximum precipitation can be in the wrong hemisphere*

In Fig. 2b (from Chao 2000), it is obvious that if the slope of line S becomes greater (i.e., if line S becomes more vertical) relative to curve R through a modification of the model physics, the two components of the double ITCZ will merge sooner (i.e., the southern ITCZ will move to merge with the northern ITCZ sooner) as the SST peak is moved north from the equator. On the other hand, if the slope of line S relative to curve R is weak enough, or the SST peak is not moved sufficiently far from the equator, the merger will not happen. For a seasonal movement of the SST peak that moves only between, for example, 5S and 10N (as the observed SST peak in the Pacific, ignoring the minor peak northeast of Australia; or as the observed zonal mean SST), a weaker slope of line S relative to curve R–by not allowing the merger to occur--yields a seasonal cycle of

[2] Although the ITCZ is not responsible for all the convective heating, it is by far the main contributor. Also, there can be net energy flux across the MCE. But since the Hadley circulation is dominant in the tropics, this flux is negligible.

the ITCZ that has a double ITCZ year-round with a stronger southern component in the JJA season. On the other hand, a greater slope of line S relative to curve R yields this ITCZ structure only in off-JJA seasons and yields a single northern ITCZ in the JJA season, when the SST peak is farthest north of the equator.

In the eastern Pacific in the JJA season, the SST has a much stronger peak in the meridional direction than in the central and western Pacific. Thus, according to our interpretation above, the wrong hemisphere problem does not occur in the eastern Pacific.

3.c *Explanation for how the simulated ITCZ maximum can remain at an equatorial location*

From Fig. 1 it is show that by changing cumulus parameterization gradually (for example, as discussed in Chao and Chen (2004) in association with their Figs. 2 and 3) curve R can be gradually changed from that in Fig. 2a to that in Fig. 2b. In between curve R--relative to line S--can take on different shapes as in Fig. 2.c. For those R curves that have substantial positive R-minus-S values just north of the equator, there is a stable intersection point at an equatorial location and if the SST peak is not moved too far away from the equator, the ITCZ can remain at an equatorial location year-round.

3.d *Remarks*

Curve R, relative to line S, in Fig. 2 can be changed as a result of changing curve B in Fig. 1 through changes in model physics. Different R (Fig. 2c), relative to line S,

gives rise to different systematic errors. Therefore, the systematic ITCZ errors can fall between the two types as described in subsections 3.b and 3.c. In both models and nature, due to regional SST distribution differences, curve R relative to line S, can be somewhat different in different regions. To minimize the systematic errors in simulating the ITCZ over the oceans, curve R--relative to line S--should be somewhat close to the solid curve in Fig. 2c, which represents the nature. If it deviates sufficiently toward the dotted line in Fig.2c the wrong hemisphere problem arises and if it deviates sufficiently toward the other direction the concentration-over-the-equator problem arises. Finally as a reminder, our study in this paper is based on concepts formed for an aqua-planet with a single SST peak. In regions over or close to land mass and regions where there are two latitudinal SST peaks our findings may need considerable modification, which we intend to study in the future.

4. Discussions

If given a GCM that has maximum ITCZ precipitation in the southern hemisphere in the central and western Pacific in the JJA season, one should be able to correct the problem by increasing the SST peak in the northern hemisphere in the JJA season or by changing the model physics such that line S becomes more vertical relative to curve R in Fig. 2b. Or, if a model has maximum ITCZ precipitation over the equator in a region when it is not supposed to be there, one should try to change the model physics such that curve R--relative to line S--is changed to be more like the solid curve in Fig. 2c. Of

course, changing the SST is not a real option, but it can verify our idea. The next question is how to change the model physics. We will discuss three possibilities.

As demonstrated in Chao and Chen (2004) curve B in Fig. 1 and therefore curve R in Fig. 2 can be changed by changing the cumulus parameterization. One way to do this, as they suggested, is to add a condition to the cumulus parameterization scheme such that the cumulus parameterization scheme is allowed to operate only when the boundary layer relative humidity exceeds a critical value. By increasing this critical value, the convection is harder to occur, but when it does occur, it is more vigorous, which means a curve B in Fig. 1 with reduced magnitude. This reduces the control of the ITCZ due to the earth's rotation--i.e., it reduces the magnitude of curve B in Fig. 1 (see the discussions associated with Figs. 11 and 14 of Chao and Chen (2004)), thus making the slope of line S relative to curve R greater in Fig. 2b. Of course, changing this critical value also affects the slope of line S. However, since curve R can be changed so drastically as to change its shape from curve R in Fig. 2b to that in Fig. 2a (as shown in experiments associated with Figs. 2 and 3 of Chao and Chen 2004), the change in the slope of line S is relatively minor. Therefore, increasing the critical boundary layer relative humidity has the effect of moving curve R, relative to line S, in Fig. 2c in the direction from the dotted curve to the long-dashed curve.

A second possible change in the model physics is to change the degree of re-evaporation of the cumulus rainfall. With rain re-evaporation intensified--which reduces the net convective heating--the synoptic-scale convective systems are less vigorous. But exactly how curve R and line S and changed by adding rain re-evaporation requires

further study. Whether rain re-evaporation should be increased or decreased so as to realize its salutary effect will have to be determined by experimentation.

A third possibility of changing the model physics is to modify the cumulus momentum transport (CMT). Intensifying CMT reduces the intensity of the synoptic-scale convective systems and should have similar, but not identical, effects as rain re-evaporation. In the next section, our explanation in the preceding section is put to the test.

Increasing horizontal resolution tends to make cumulus convection more concentrated; i.e., making the horizontal scale of the convection smaller. (This is due to the unfortunate fact that resolution dependent physical parameterization schemes have not yet been developed. In other words, changing horizontal resolution effectively changes physical parameterization.) Since curve B in Fig. 1 is inversely related to the square of the horizontal scale of the convective circulation (Curve B is the latitudinal gradient of $\alpha^2 N^2$, where α is the ratio of the vertical scale to the horizontal scale of the convective circulation and N^2 is the vertical stability. See Chao and Chen (2004) for details), increasing horizontal resolution increases α and thus the magnitude of curve B in Fig. 1 and in turn has the effect of moving curve R in Fig. 2c in the direction from the long-dashed curve toward the dotted curve. This is consistent with Sumi's (1992) finding that, in an aqua-planet model with uniform SST and horizontally uniform net radiative heating, increasing horizontal resolution turned a single ITCZ over the equator into a double ITCZ straddling the equator. This explains why GCMs behave very differently and require re-tuning when the horizontal resolution is changed. In the future when resolution dependent physical parameterizations are developed, this kind of model

behavior should cease. See Jung and Arakawa (2004) for further discussions on resolution dependent physical parameterizations. The effects of changing vertical resolution remain to be explored.

Of course, there can be many other ways of modifying the model physics to change the slope of line S relative to curve R in Fig. 2b; the mechanisms of how they effect their changes remains to be explored. Also, for the three possible ways of changing the model physics we just discussed each may have its own side effects. For example, intensifying rain re-evaporation may yield excessive relative humidity at low levels. Thus the final solution has to be a combination of several modifications to the model physics.

5. Supporting experiments

The model used for this study is a recent version of the Goddard Modeling and Assimilation Office's (GMAO) Earth Observing System (GEOS-5) GCM. The model has the finite-volume dynamical core of Lin (2004), the combined boundary layer and turbulence package of Louis (1980) and Lock et al. (2000), the land surface model of Koster and Suarez (1996), the radiation package of Chou and Suarez (1994, 1999), the relaxed Arakawa-Schubert scheme (RAS, Moorthi and Suarez 1992), and the prognostic cloud scheme of Bacmeister et al. (2006). It also has the rain re-evaporation scheme of Bacmeister et al. (2006). The scheme of cumulus transport of momentum advects momentum using the cumulus mass flux calculated in RAS. The resolution we used was 2.5° (lon), 2° (lat), and 32 levels.

We created an aqua-planet version of GEOS-5 and used it and the full model for our experiments. We did ten one-year experiments, APE1 through APE10, with the AP model; in each experiment the rain re-evaporation scheme was multiplied by a factor EV and the cumulus momentum transport was multiplied by a factor CF. EV varies from 0 to 2; 0 means rain re-evaporation is not used and 1 means the original rain re-evaporation intensity is used. CF is either 1 or 0--i.e., cumulus momentum transport is either used or not used (see Table 1a).

In all these experiments, the initial condition is the end result of a three-year AP experiment with globally- and temporally-uniform SST (29°C) and solar angle Z (cosZ=0.25), starting from a resting atmosphere plus minute perturbations in surface winds, uniform surface pressure and temperature and moisture fields as functions of height only. This initial condition, given a date of January 1, has a double ITCZ. Also, the SST is a linear combination of 25% of a constant 29°C and 75% of a Gaussian latitudinal profile centered at the equator as specified in Chao (2000, see its Eq. 1). In APE1 through APE10 the SST remains unchanged in the first 4 months and then the SST latitudinal profile, retaining its shape, is moved northward by 15 degrees in 8 months at a constant rate.

Figs. 3a and 3b show the zonally-averaged precipitation rate as a function of latitude and time for APE2 and APE7, respectively. Fig. 3a shows that as the SST peak is moved poleward from the equator, the ITCZ behaves just like in Fig. 2a—falling behind the SST peak at first and then catching up with it, but failing to do so completely and then remaining almost stationary in spite of further poleward movement of the SST peak, essentially a repeat of the experiment described in Fig. 2 of Chao (2000). In APE3

through APE5, during the first four months while the SST peak is at the equator, a double ITCZ exists and the two components of the double ITCZ draw closer as the rain re-evaporation rate is increased. The change from a single ITCZ in APE2 to a double ITCZ in APE3 in the first four months of the experiments indicates that curve R in Fig. 2b has a small magnitude so that it intersects line S only at the equator in APE2, whereas it has a larger magnitude so that it intersects line S at three places in APE3. The difference between APE2 and APE3 is due to a change in the intensity of rain re-evaporation.

Table 1b gives 1) the month that the southern component of the double ITCZ crosses the equator, 2) a label "single" for experiments yielding a single ITCZ, or 3) a label "double" for an experiment yielding double ITCZ but its southern component did not cross the equator. In APE3 through APE5, as the SST peak is moved northward, the southern ITCZ intensifies and its crossing into to the northern hemisphere occurs later when the rain re-evaporation rate is increased—results of decreasing of the slope of curve S relative to curve R in Fig. 2b. These experiments lend support to our interpretation of the mechanism behind the ability of rain re-evaporation to influence the ITCZ simulation in GCMs.

Table 1b shows that inclusion of cumulus momentum transport can delay the equator-crossing of the southern component of the double ITCZ--i.e., decreasing the slope of line S relative to curve R in Fig. 2b for EV=0.7 and 1 cases. However, for EV>1 the impact of adding cumulus momentum transport is reversed. Thus, like rain re-evaporation, the impact of cumulus momentum transport on the ITCZ location is not uniform. Also, when cumulus momentum transport is included, a further increase of EV

above 1 does not delay the merger. This indicates that both curve R and line S in Fig. 2b increase at a rate to balance each other.

In summary, these AP model experiments demonstrate the highly nonlinear response of the ITCZ behavior to changes in rain re-evaporation and cumulus momentum transport. They also illustrate the complexity of correcting the ITCZ systematic errors.

We also did four experiments with the full model at 2.5° (lon) by 2° (lat) and 72 levels of resolution (which is more than double the vertical resolution in both the troposphere and stratosphere as used in the AP experiments): FME1 with no rain re-evaporation (EV=0); FME2 with rain re-evaporation (EV=1); FME3, a repeat of FME1 but with an SST perturbation in the form of a linear function of latitude from zero at the equator to 4°C at 20°N, and another linear function back to zero at 40°N being added to the observed SST used in FME1 in the JJA season; FME4 a repeat of FME2 with a condition on RAS that the boundary layer relative humidity has to be greater than 95%. In all four experiments, CF is set at 1.

The full model experiments started from Oct 30, 1992 using observed SST. Each ran for two years. FME1 show a problem of ITCZ precipitation peak in the wrong hemisphere only in the limited range of 135E to 170E in the JJA season (Fig. 4a and 4b). This problem does not occupy a longitudinal range as wide as that in the NSIPP model before rain re-evaporation was introduced (Fig. 1a of Bacmeister et al. 2006.) The NSIPP model showed a stronger JJA ITCZ peak south of the equator in the longitudinal range of 100E to 135E than in the region to the east; but this problem does not exist in GEOS-5. In this longitudinal range the SST peak in the JJA season is at about 17N. Such high SST peak latitude is favorable for excessive ITCZ precipitation south of the

equator if curve R in Fig. 2b is sufficiently large relative to line S, as explained in subsection 3.b. Apparently this is not happening in GEOS-5. In the longitudinal range between 135E and 170E the maximum ITCZ precipitation is in the equatorial region. From 170E to 110W FME1 shows a stronger SPCZ than the ITCZ north of the equator over central Pacific in JJA. This corresponds well to observations. Between 160W and 120W there are two SST latitudinal peaks with the southern one somewhat stronger. Apparently, the SST control is somewhat stronger than the rotational control in FME1 and thus the SPCZ is stronger than the ITCZ north of the equator. At this time we do not have an explanation for this, since our explanations thus far are only based on single-peak SST latitudinal distribution. FME2 shows that the strength of the SPCZ has been reduced to some extent in 1994. Notice that the 4 mm/day contour line in the SPCZ has retreated considerably toward northwest in FME2 (Fig. 5.b) as compared with FME1 (Fig. 4.b). But no similar change is found in 1993 (Figs. 4.a and 5.a). In summary the type of wrong hemisphere problem as explained in Subsection 3.b is not occurring in FME1 and FME2.

The precipitation maximum in the eastern half of the Indian Ocean in FME1 and FME2 in the JJA season in 1993 and 1994 fails to reach Bay of Bengal and is controlled by local SST maximum. In the western half of the Indian Ocean the precipitation maximum resides at an equatorial latitude in both FME1 and FME2, although it is reduced somewhat in FME2. The cause of this equatorial location has been offered in Subsection 3.c. The weak JJA precipitation in the northern Indian Ocean in FME1 has persisted in FME2. In the DJF season both FME1 and FEM2 also show similar problem in the Indian Ocean, with the exception of FME1 in DJF of 1993-94, where there is a double ITCZ in the eastern Indian Ocean. Thus, rain re-evaporation is not a panacea and

has to be used in conjunction with other changes in the GCM physics. In summary the version of the GEOS-5 model with the particular resolution we used has a curve R, relative to line S, that deviates from the solid line in Fig. 3c toward the two dashed lines; unlike the NISPP model (before rain re-evaporation was added), which has a curve R deviating toward the dotted line.

In separate experiments with the same model but with horizontal resolution doubled the wrong hemisphere problem arises without rain re-evaporation and the problem is alleviated with rain re-evaporation (Figs. 6a and 6b). The arise of the wrong hemisphere problem as a result of increasing horizontal resolution is consistent with our discussion on the effect of increasing horizontal resolution in the preceding section. The fact that rain re-evaporation helps to alleviate the wrong hemisphere problem in the higher horizontal resolution experiments indicates that the effect of rain re-evaporation is very much horizontal resolution dependent. The mechanism behind this dependence remains to be explored.

FME3 (Fig. 7) shows that strengthening the northern SST peak and moving it further north in the JJA season can move the ITCZ to the northern hemisphere in JJA. This is consistent with our AP experiments and it supports our interpretation as presented in the preceding paragraph.

In FME4 (Fig. 8) the ITCZ precipitation shows no sign of double ITCZ, except a small region around 170°W, as a result of curve R in Fig. 2.b being reduced and there is only one intersecting point either near the equator when the SST peak is near there, as in the western Pacific and the Indian Ocean, or about 10°N when the SST peak is near 10°N, as in the eastern Pacific and the Atlantic.

6. Summary and remarks

The latitudinal location of the ITCZ over the oceans is controlled by the balance of two factors: the latitudinal distribution of the SST and the earth's rotation. The strength of each factor is affected by the model physics. Thus, the latitudinal location of the ITCZ responds to changes in the model physics. Identification of the origin of some of the ITCZ systematic errors and a description of how the treatment of the moist convective process can affect these errors have been the contribution of this paper and the work leading to it. Also, the impacts on the ITCZ systematic errors due to changes in rain re-evaporation and cumulus momentum transport are highly variable. The ITCZ simulation can also be sensitive to other components of the model physics (Chao and Chen 2004). However, they have not yet been systematically studied yet.

If the SST-peak controlling factor is greater than the rotational controlling factor, the ITCZ precipitation in a zonally non-uniform setting tends to show excessive peaks in the zonal direction, in addition to the meridional direction, generating locally excessive precipitation maximum areas. Many GCMs show a dip in the ITCZ precipitation in the zonal direction in the middle of the eastern Pacific for this reason—that the control by the SST peak in the Pacific coastal region next to Central America is too high. Similar symptoms can also show up in equatorial Indian Ocean and western Atlantic (Figs. 4.a, b). Also, the JJA mean precipitation maximum in the northwestern equatorial Pacific is often excessive for the same reason. As shown in Fig. 7, the higher control of SST peak, relative to the rotational control, worsens the problem of excessive ITCZ precipitation

concentration over local SST maxima in the equatorial regions. Thus, an obvious way to alleviate this problem is to reduce the SST peak control by making the condition for the occurrence of parameterized cumulus convection less restrictive. Exactly how to accomplish this requires further study.

The response to a change, or a set of changes, in the model physics can be very different, or even in the opposite directions in different areas, due to different regional and temporal SST distributions. For example, Figs. 5.a and 5.b have demonstrated that adding rain re-evaporation could help alleviate the wrong hemisphere problem in western and central Pacific in one year but not in another year. This is because the SST distribution in these areas is different in the different years.

How to change the GCM physics so as to improve the ITCZ precipitation simulation remains a challenge, despite the conceptual advances made herein. Although we have identified a few factors in the model physics that may influence the simulation of the ITCZ precipitation, we do not yet have a complete collection of these factors. Also, we have not completely explained the mechanisms behind their influences. Moreover, our interpretation of their influences, as presented in Section 4, centers on their impact on the intensity of the synoptic-scale convective systems; there may be other aspects of the synoptic systems, such as size and life cycle, that can be changed by changing these factors. Among the few important factors that we are familiar with we do not yet know to what degree each of them should be changed. There may be sets of changes to these factors that can bring similar degree of improvement in the ITCZ precipitation simulation. The best choice within these sets of changes may have to be determined by--in addition to the model's performance in simulating the monthly and

seasonal mean structure of the ITCZ--the model's performance in simulating phenomena related to the ITCZ, such as the Madden-Julian oscillation, mixed Rossby-gravity (Yanai) waves, Kelvin waves, and the ITCZ breakdown-and-zonalization cycle (all related to the oscillations of the convection within the ITCZ). Thus, the physical mechanisms behind these other tropical phenomena should also be studied in order to improve the GCM simulation of the ITCZ precipitation. In other words, possible sources of the systematic errors in the GCM tropical circulation simulation in the wave number-frequency domain and the mechanisms behinds them should also be studied. Thus, much more work still lies ahead.

Although the recent effort in super-parameterization has resulted in improvement in the ITCZ precipitation simulation, there is room for further improvement. For example, the too-high precipitation maximum in the northwestern Pacific in JJA is still present in the latest models with super-parameterization (Tao, personal communication).

This study is based on aqua-planet settings with prescribed SST; the roles of land-atmosphere and ocean-atmosphere interactions in determining ITCZ precipitation will be among our future research topics. Many ITCZ precipitation problems related to landmass and air-sea interaction await our effort. For example, the coastal regions of South America and India are often the trouble spots for GCM precipitation simulation. The missing ITCZ in the African coastal region from Guinea to Nigeria, which may be related to the precipitation over-concentration in the western Atlantic, in Figs. 4.a and 4.b is another example. Improving the El Nino simulation, which strongly depends on the ITCZ simulation, remains a challenge as well.

Acknowledgments

This work was supported by the Modeling, Analysis and Prediction program of NASA Science Mission Directorate.

References

Bacmeister, J. T., M. J. Suarez, and F. R. Robertson, 2006: Rain re-evaporation, boundary-layer/convection interactions, and Pacific rainfall patterns in an AGCM. *J. Climate*. In press.

Chao, W. C., 2000: Multiple quasi-equilibria of the ITCZ and the origin of monsoon onset. *J. Atmos. Sci.*, **57**, 641-651.

Chao, W. C., and B. Chen, 2001: Multiple quasi-equilibria of the ITCZ and the origin of monsoon onset. Part II. Rotational ITCZ attractors. *J. Atmos. Sci.*, **58**, 2820-2831.

Chao, W. C. and B. Chen, 2004: Single and double ITCZ in an aqua-planet model with constant SST and solar angle. *Climate Dynamics*, **22**, 447-479.

Chou, M. D. and M. J. Suarez, 1994: An efficient thermal infrared radiation parameterization for use in general circulation models. NASA Tech. Memo, 104606, **10**, 84pp.

Chou, M. D. and M. J. Suarez, 1999: A solar radiation parameterization for atmospheric studies, NASA Technical Memo, 104606, Vol. 11, 40pp.

Hack, J. J., J T. Kiehl and J. W. Hurrell, 1998: The hydrologic and thermodynamic characteristics of the NCAR CCM3. *J. Clim.*, **11**, 1179-1206.

Jung, J. H. and A. Arakawa, 2004: The resolution dependence of model physics: Illustration from nonhydrostatic model experiments. *J. Atmos. Sci.*, **61**, 88-102.

Koster, R., and M. Suarez, 1996: Energy and water balance calculations in the Mosaic LSM. *NASA Tech Memo.* 104606, Vol. 9, 60 pp. (available from the library of NASA/Goddard Space Flight Center, Greenbelt, MD 20771).

Lin, S.-J. 2004: A "vertically Lagrangian" finite-volume dynamical core for global models. *Mon. Wea. Rev.,* **132**, 2293–2307.

Lindzen, R. S. and S. Nigam, 1987: On the role of sea-surface temperature gradients in forcing low-level winds and convergence in the tropics. *J. Atmos. Sci.*, **44**, 2418-2436.

Lock, A. P., A. R. Brown, M. R. Bush, G. M. Martin, and R. N. B. Smith: 2000: A new boundary layer mixing scheme. Part I: Scheme description and single-column model tests. *Mon. Wea. Rev.*, **128**, 1387-1399.

Louis, J.-F., 1979: A parametric model of vertical eddy fluxes in the atmosphere. *Boundary Layer Meteor.* **17**, 187-202.

Manabe, S., J. Smagorinsky and R. F. Strickler, 1965: Simulated climatology of a general circulation model with a hydrological cycle. *Mon. Wea. Rev.*, **93**, 769-798.

Moorthi, S., and M. J. Suarez, 1990: Relaxed Arakawa-Schubert: A parameterization of moist convection for general circulation models. *Mon. Wea. Rev.,* **120**, 978-1002.

Raymond, D. J. 2000: The Hadley circulation as a radiative-convective instability. *J. Atmos. Sci.*, **57**, 1286-1297.

Sumi, A. 1992: Pattern formation of convective activity over the aqua-planet with globally uniform sea surface temperature. *J. Meteor. Soc. Japan*, **70**, 855-876.

Wu, X., X. Liang, and G. J. Zhang, 2003: Seasonal migration of ITCZ precipitation across the equator: Why can't GCMs simulate it? *GRL*, **30**, No. 15, 1824-1828.

Zhang, G. J. and H. Wang, 2006: Toward mitigating the double ITCZ problem in NCAR CCSM3. *Geophys. Res. Let.*, **33**, L060709, Doi:10.1029/2005GL025229.

Appendix

The additive assumption in Fig. 2

In Fig. 2 it is assumed that the two types of attractions on the ITCZ due to the earth's rotation and the SST peak can be added. This additive assumption is only approximately correct. Our explanation does not hinge on this assumption being exactly correct. This appendix provides a discussion of this point.

The ITCZ latitudinal location can be expressed as the latitude(s) where $A(\Omega,SST,\phi)=0$ and $\partial A/\partial\phi>0$, where A denotes the net southward attraction on the ITCZ. A is of course a highly nonlinear function of the earth's rotation rate Ω, SST distribution, and latitude ϕ, among other factors. This equation can only be approximately expressed as $A(\Omega, G, \phi) + A(0, SST, \phi)=0$, where G is the globally averaged SST—or curve R minus line S=0 in Fig. 2.

Our argument in explaining Fig. 3 of Chao and Chen (2001) using Fig. 2b only requires that as the SST peak is moved northward from the equator, the two ITCZ components move northward also. The locations of these ITCZ components do not have to be at the exact locations of the intersecting points between curve R and line S in Fig 2. It is obvious that when the SST peak is moved northward from the equator, both ITCZ components should move northward as well. Our argument as to why the southern ITCZ component should be stronger once the SST peak moves into the northern hemisphere does not depend on the additive assumption being exactly correct. We should also note

that if the additive assumption was exact, the southern ITCZ component would not reach the equator in Fig. 3 of Chao and Chen (2001).

Table 1a

	EV					
	0	0.5	0.75	1.0	1.5	2.0
CF						
0	APE1	APE2	APE3	APE4	APE5	
1		APE6	APE7	APE8	APE9	APE10

Table 1a shows the experiment labels as functions of EV and CF

Table 1b

	EV					
	0	0.5	0.75	1.0	1.5	2.0
CF						
0	single	single	June	Aug	double	
1		single	Aug	Sept	Sept	Sept

Table 1b shows the structure of the ITCZ for different experiments. Single (double) means the ITCZ remained single (double) throughout the experiment. Month means the month that the southern component of the double ITCZ crosses the equator.

Figure Captions

Fig. 1 Schematic diagram showing the strength of the two types of attraction acting on the ITCZ, both due to the earth's rotation. Curve A represents the strength of the southward attraction due to inertial stability. Curve B represents the strength of the northward attraction due to latitudinal gradient of f-modified surface fluxes associated with synoptic-scale convective systems. (From Chao and Chen 2004)

Fig. 2.a Curve R represents the net southward attraction on the ITCZ due to the earth's rotation--i.e., the difference between the two curves in Fig. 1 when MCA is used--and line S represents the northward attraction on the ITCZ due to the SST peak. Line S1 is line S when the SST peak is close to the equator. (From Chao 2000)

Fig. 2.b Curve R represents the strength of the southward net attraction on the ITCZ due to the earth's rotation--i.e., the difference between the two curves in Fig. 1--when RAS is used and line S is the strength of the northward attraction on the ITCZ due to the SST peak when the SST peak is at the equator. (From Chao 2000)

Fig. 2.c Curve R, relative to line S, has different shapes corresponding to various magnitudes of curve B in Fig. 1. The solid curve R represents that of the nature.

Fig. 3.a Zonally averaged precipitation (mm/day) for APE2 as a function of latitude and time.

Fig. 3.b Zonally averaged precipitation (mm/day) for APE7 as a function of latitude and time.

Fig. 4.a June-July-August mean precipitation (mm/day) in 1993 for FME1.

Fig. 4.b June-July-August mean precipitation (mm/day) in 1994 for FME1.

Fig. 4.c December-January-February mean precipitation (mm/day) in 1993 for FME1.

Fig. 4.d December-January-February mean precipitation (mm/day) in 1994 for FME1.

Fig. 4.e June-July-August mean surface temperature (K) in 1993 for FME1.

Fig. 4.f June-July-August mean surface temperature (K) in 1994 for FME1.

Fig. 5.a June-July-August mean precipitation (mm/day) in 1993 for FME2.

Fig. 5.b June-July-August mean precipitation (mm/day) in 1994 for FME2.

Fig. 5.c December-January-February mean precipitation (mm/day) in 1993 for FME2.

Fig. 5.d December-January-February mean precipitation (mm/day) in 1994 for FME2.

Fig. 6.a June-July-August mean precipitation (mm/day) in 1995 for Fig. 7 June-July-August mean precipitation (mm/day) in 1993 for FME3.

Fig. 8 June-July-August mean precipitation (mm/day) in 1993 for FME4.

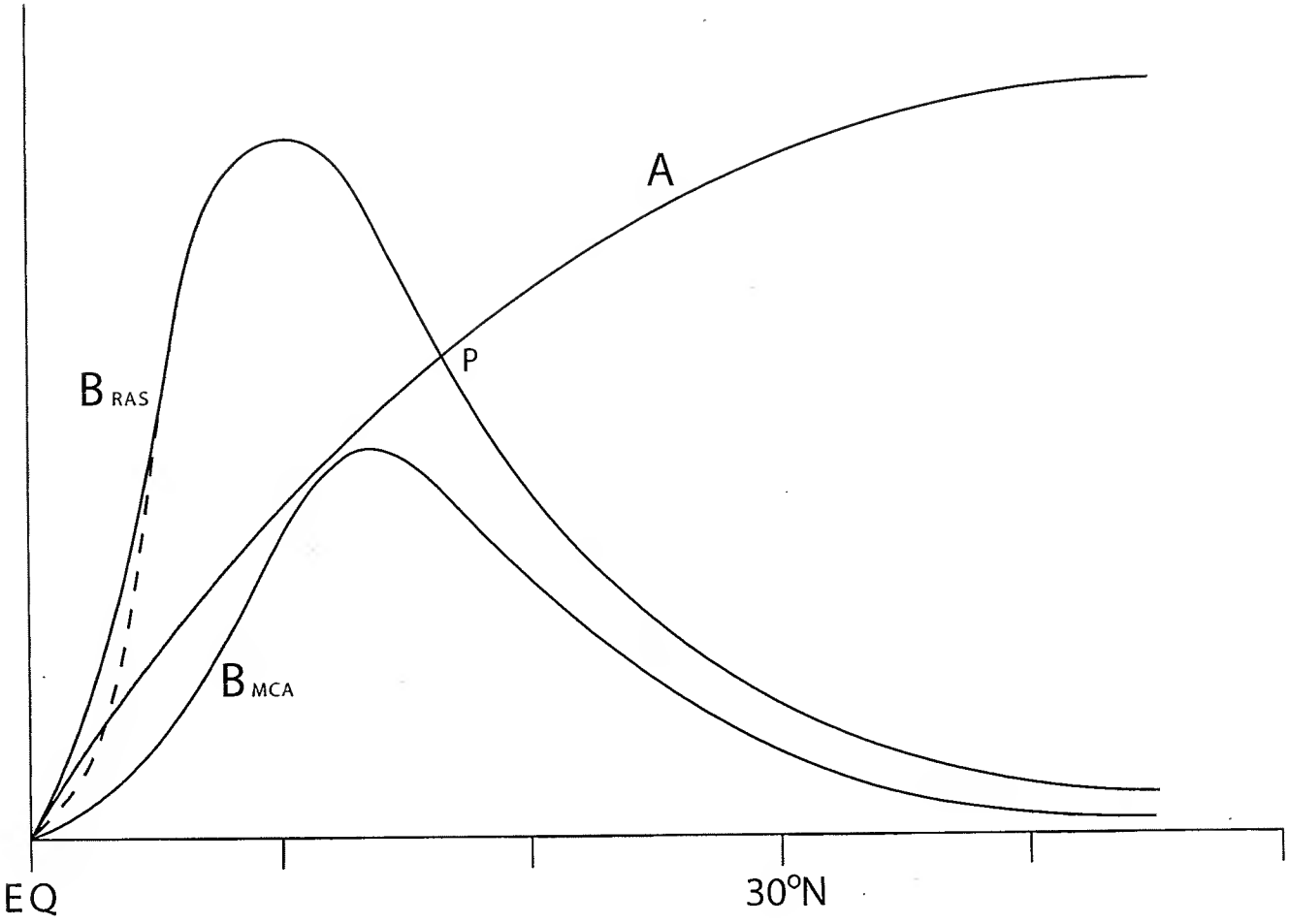

Fig. 1 Schematic diagram showing the strength of the two types of attraction acting on the ITCZ, both due to the earth's rotation. Curve A represents the strength of the southward attraction due to inertial stability. Curve B represents the strength of the northward attraction due to latitudinal gradient of f-modified surface fluxes associated with synoptic-scale convective systems. (from Chao and Chen 2004)

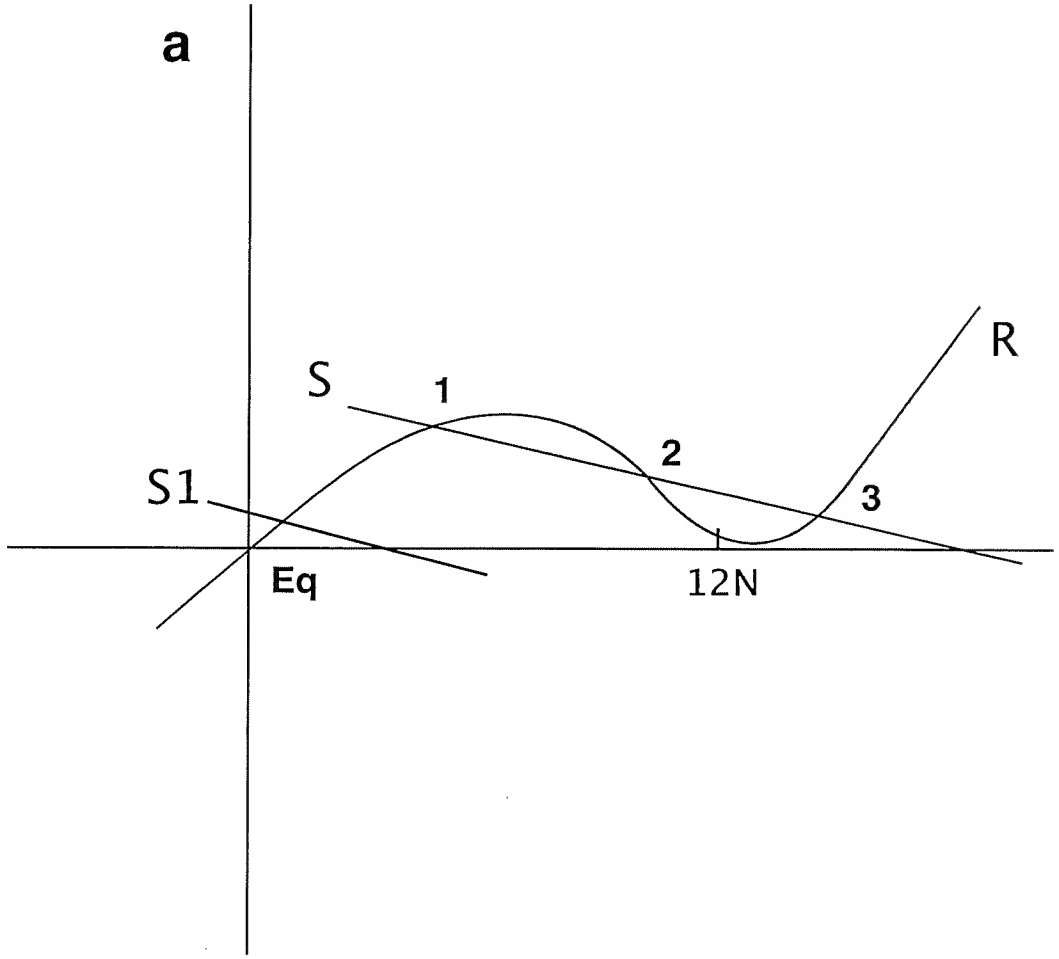

Fig. 2a Curve R represents the net southward attraction on the ITCZ due to the earth's rotation--i.e., the difference between the two curves in Fig. 1 when MCA is used--and line S represents the northward attraction on the ITCZ due to the SST peak. Line S1 is line S when the SST peak is close to the equator. (From Chao 2000)

A1408.004

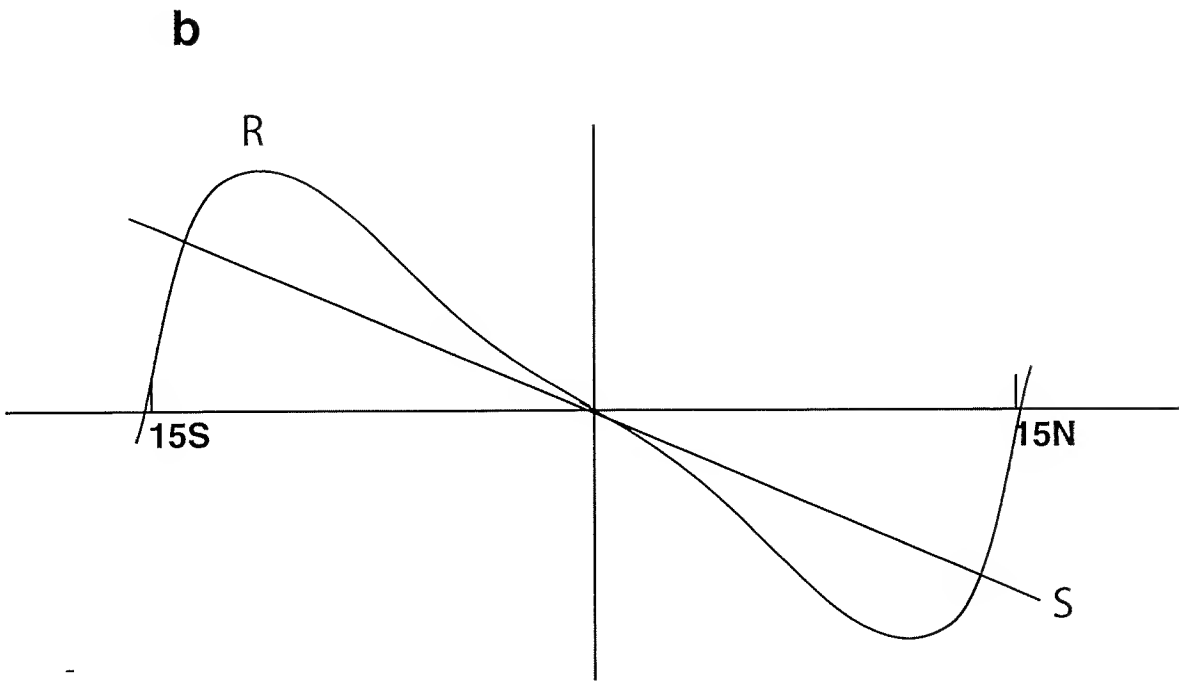

Fig. 2b Curve R represents the strength of the southward net attraction on the ITCZ due to the earth's rotation--i.e., the difference between the two curves in Fig. 1--when RAS is used and line S is the strength of the northward attraction on the ITCZ due to the SST peak when the SST peak is at the equator. (From Chao 2000)

A1408.03a

C

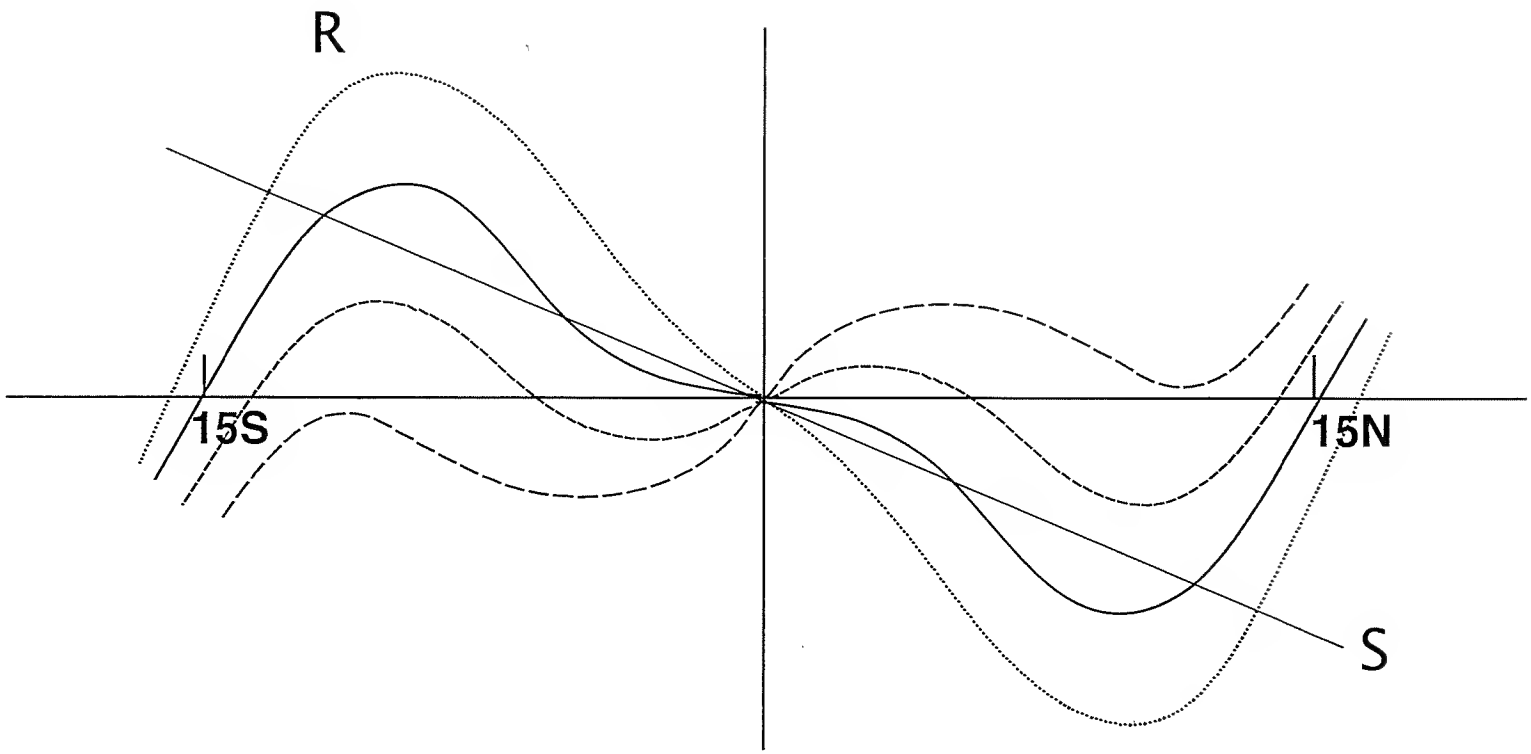

Fig. 2c Various shapes for curve R corresponding to various magnitudes of curve B in Fig. 1. The long-dashed curve corresponds to curve R in Fig. 2.a. The dotted curve corresponds to curve R in Fi.g 2.b.

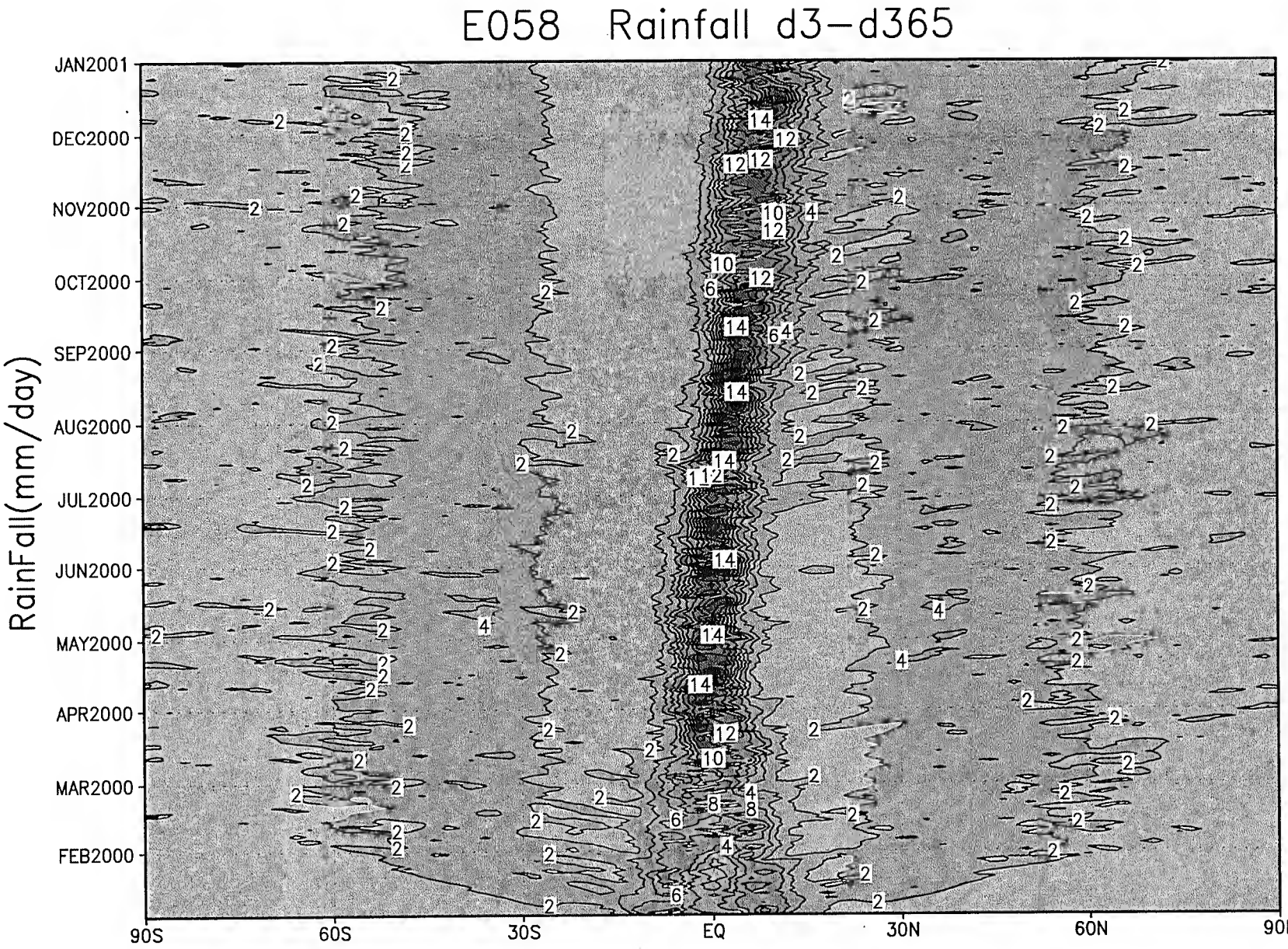

Fig. 3a Zonally averaged precipitation (mm/day) for APE2 as a function of latitude and time.

GrADS: COLA/IGES

2005–10–21–17:00

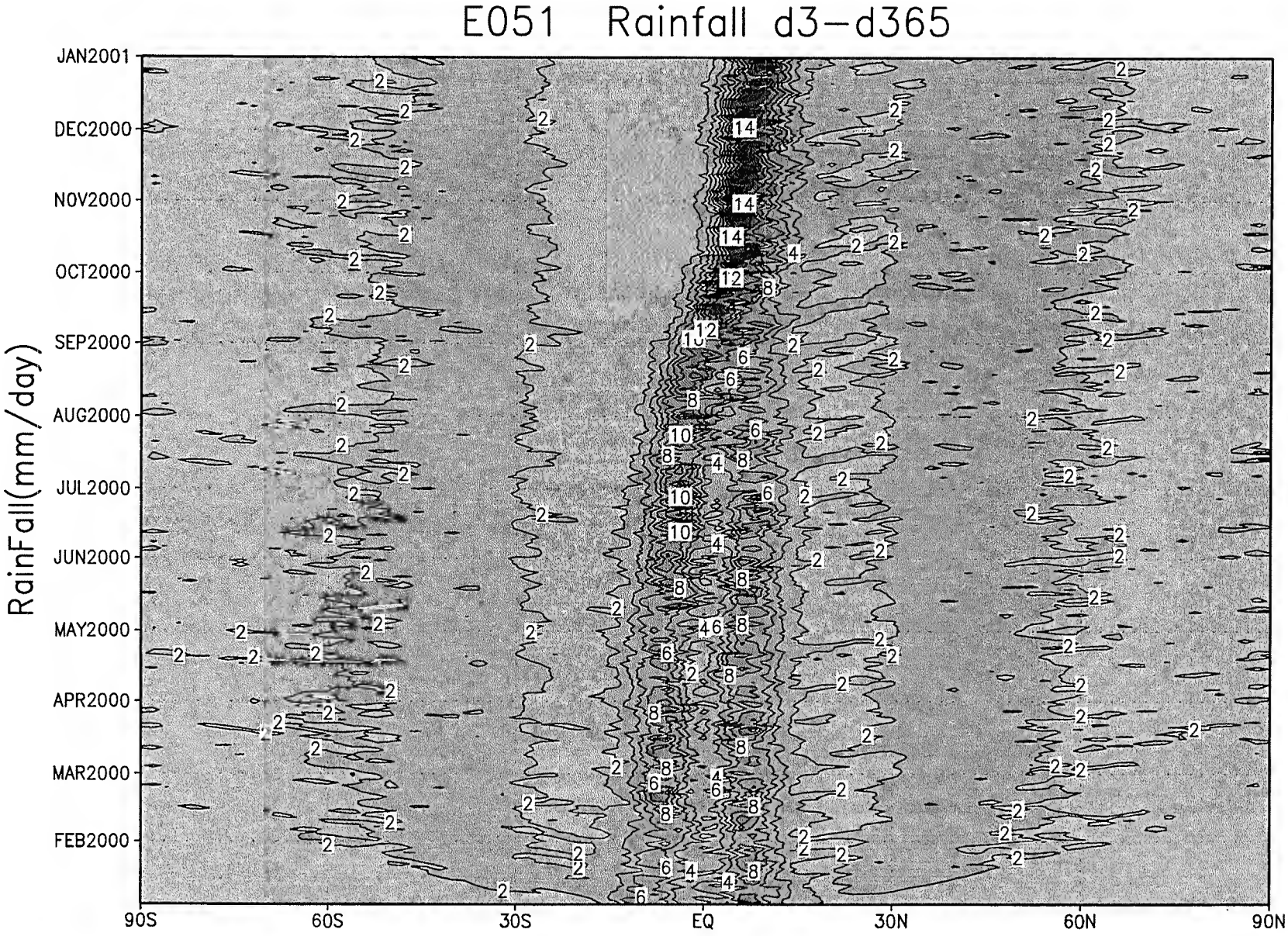

Fig. 3.b Zonally averaged precipitation (mm/day) for APE7 as a function of latitude and time.

GrADS: COLA/IGES

2005–10–17–11:11

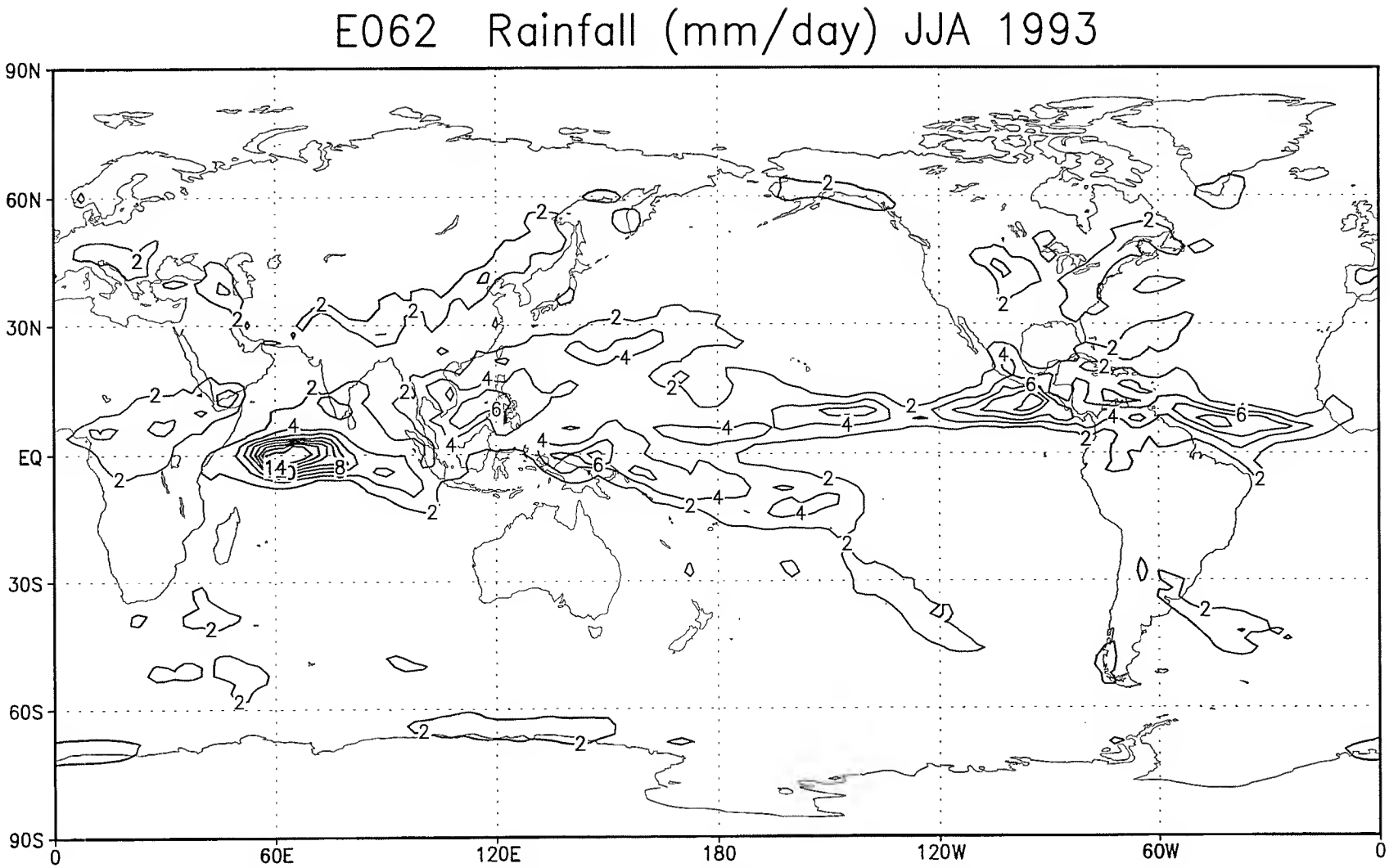

Fig. 4.a June-July-August mean precipitation (mm/day) in 1993 for FME1.

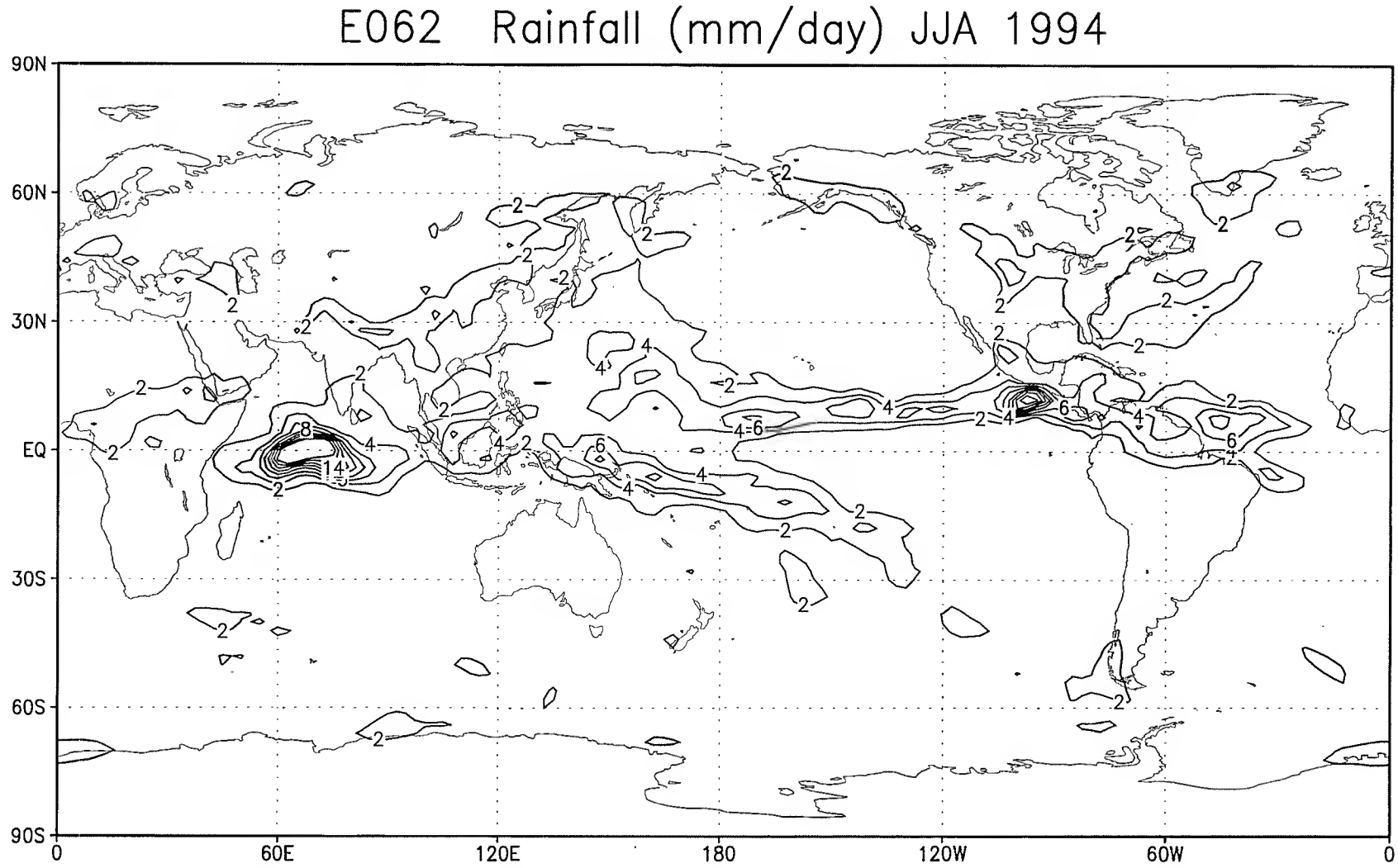

Fig. 4.b June-July-August mean precipitation (mm/day) in 1994 for FME1.

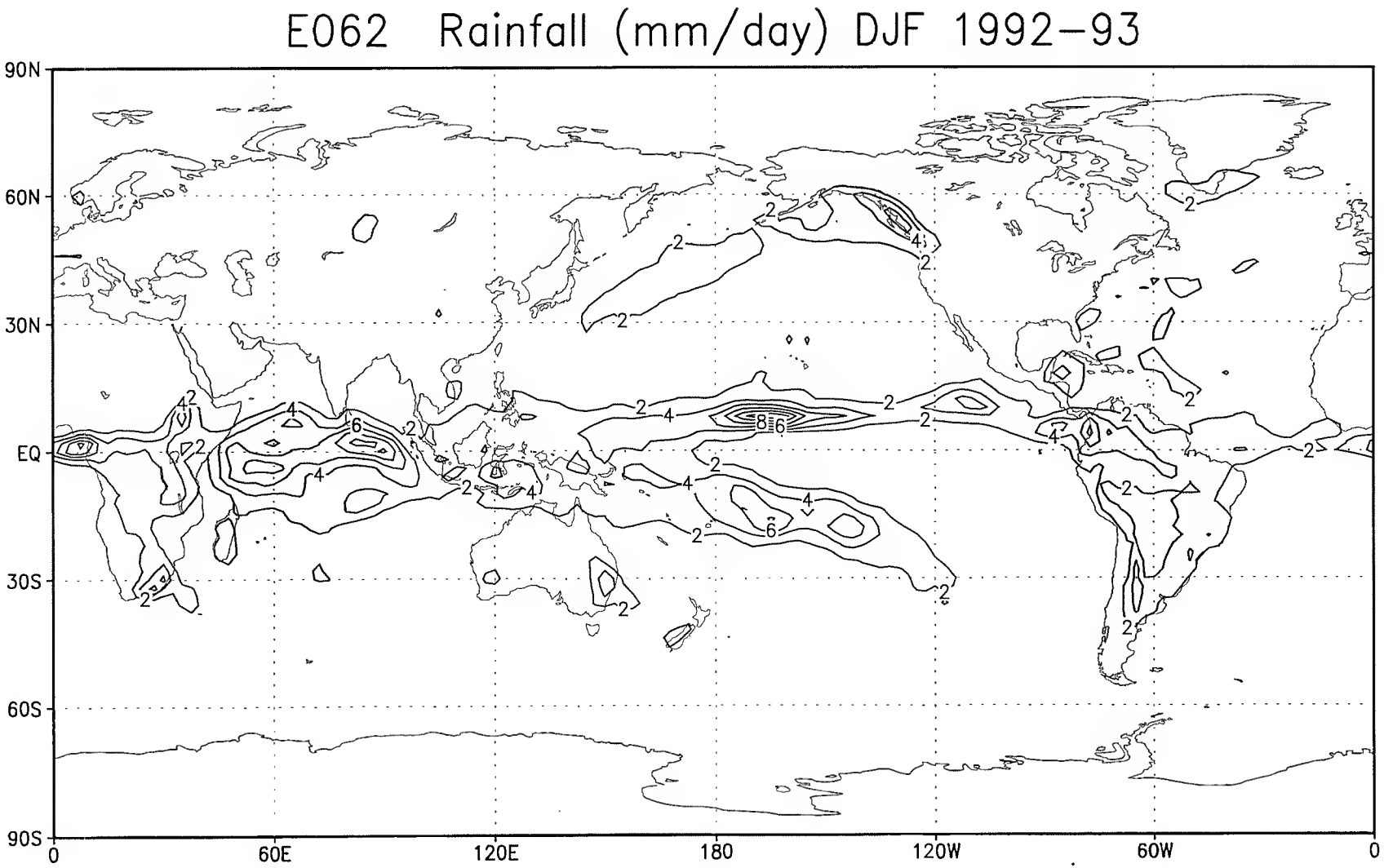

Fig. 4.c December-January-February mean precipitation (mm/day) in 1992-93 for FME1.

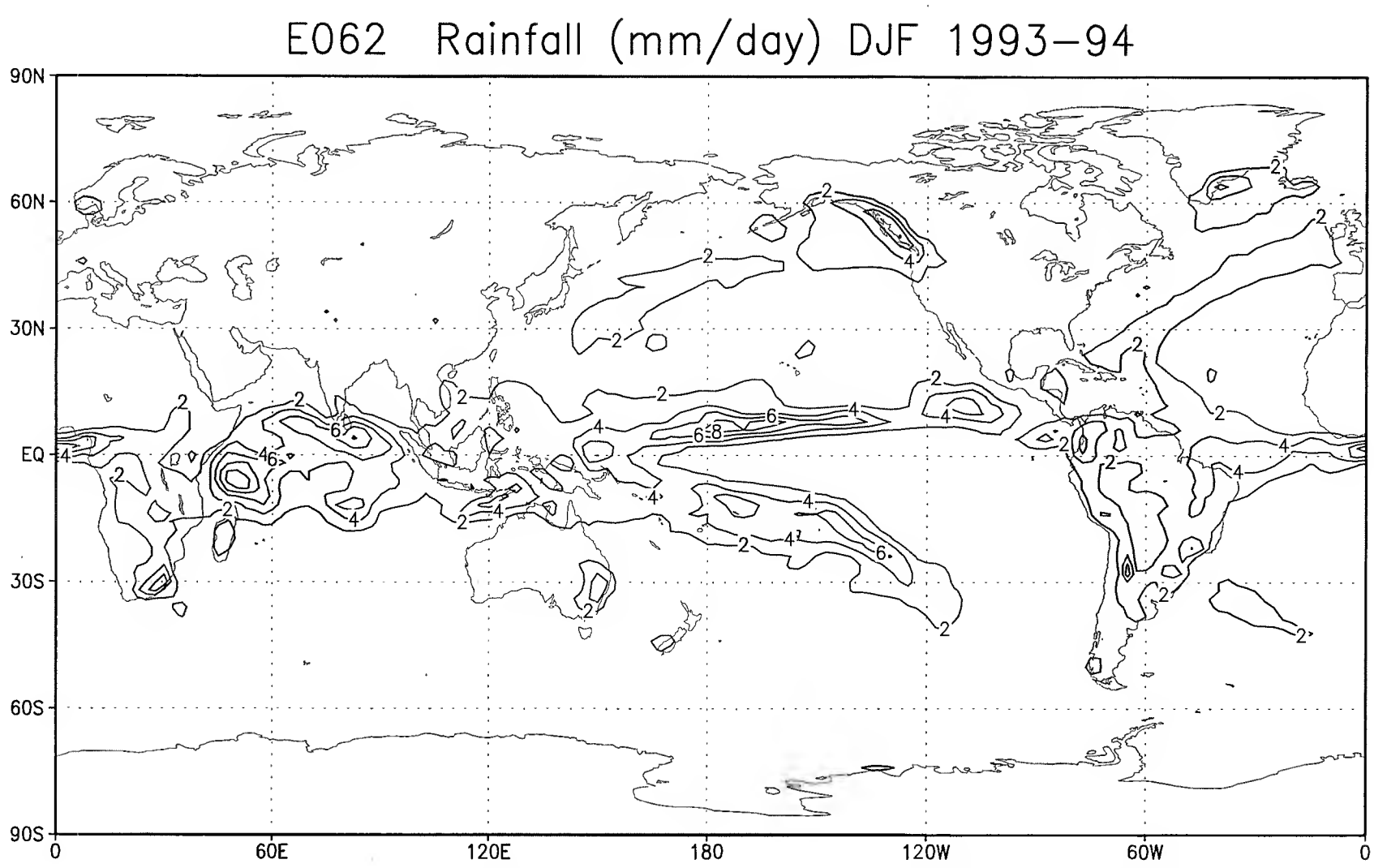

Fig. 4.d December-January-February mean precipitation (mm/day) in 1993-94 for FME1.

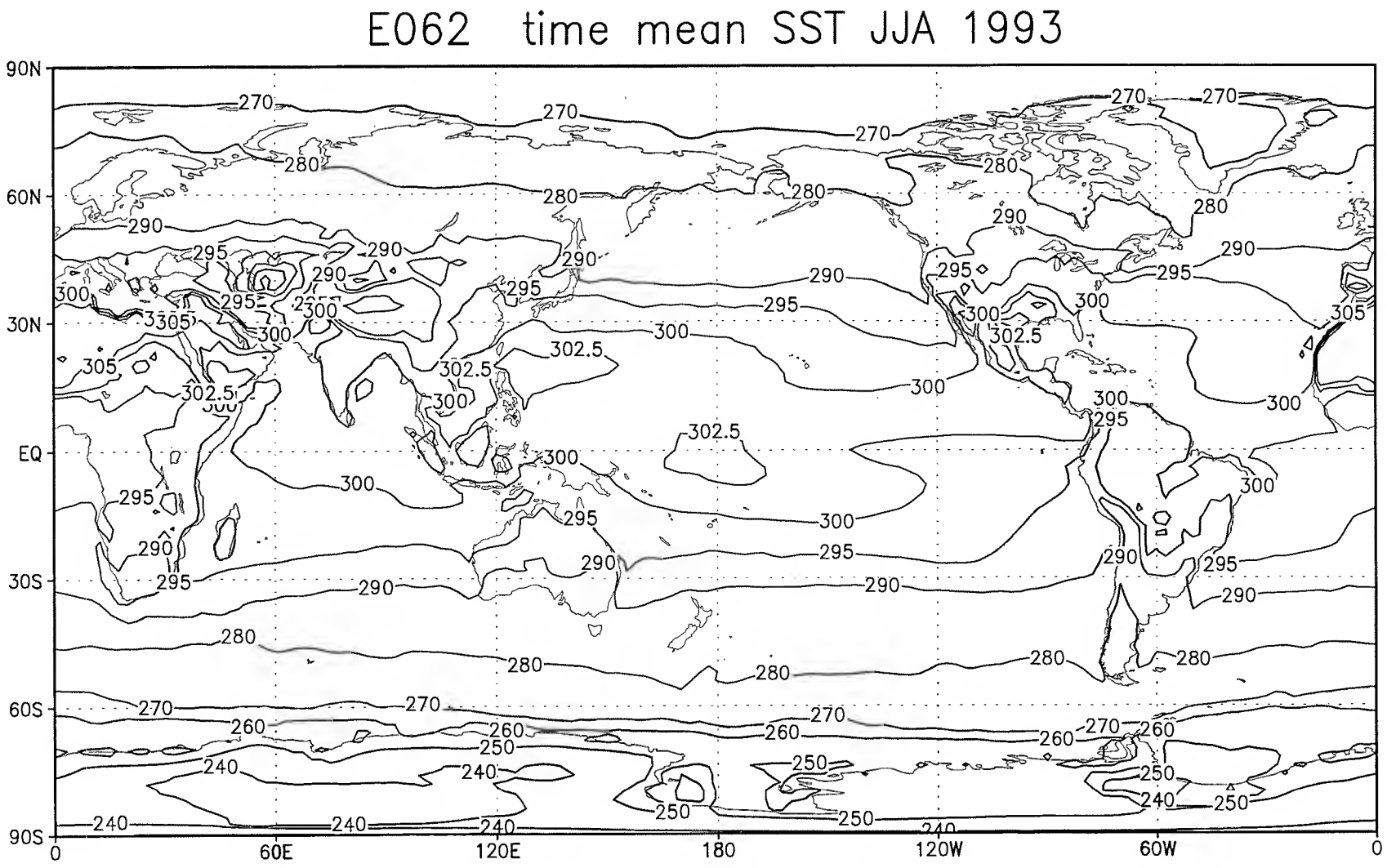

Fig.. 4e June-July-August mean surface temperature (K) in 1993 for FME1.

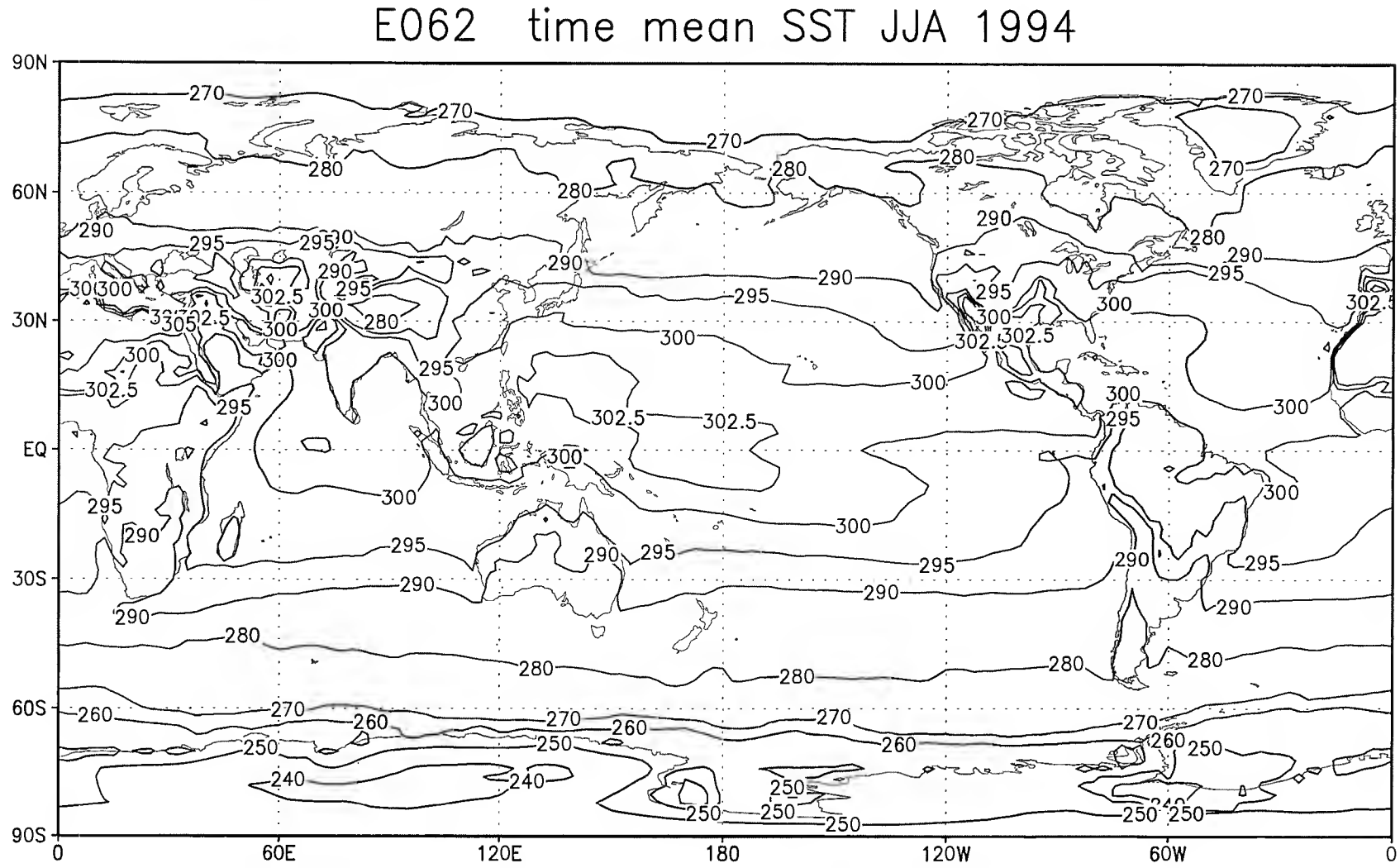

Fig. 4f June-July-August mean surface temperature (K) in 1994 for FME1.

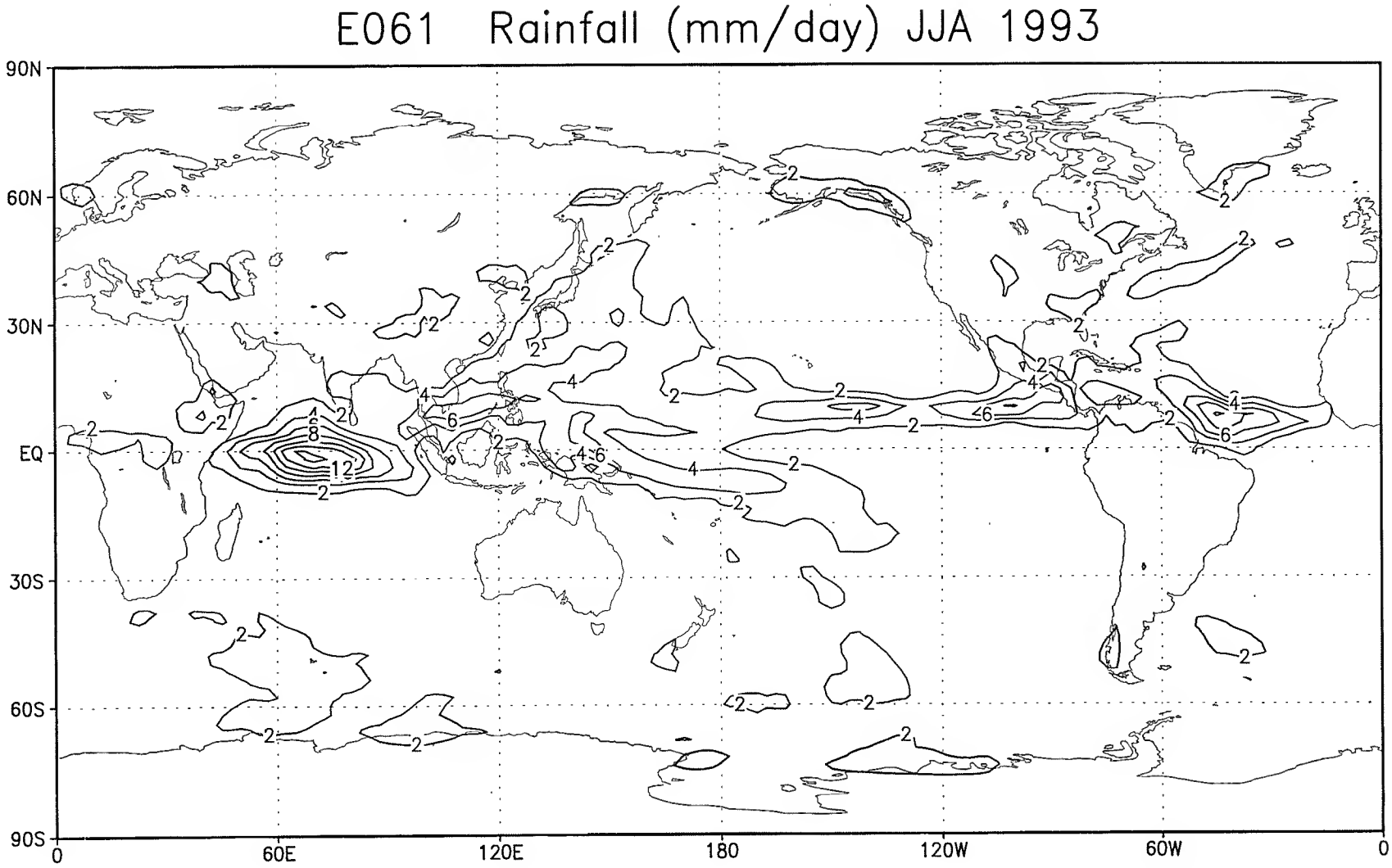

Fig. 5.a June-July-August mean precipitation (mm/day) in 1993 for FME2.

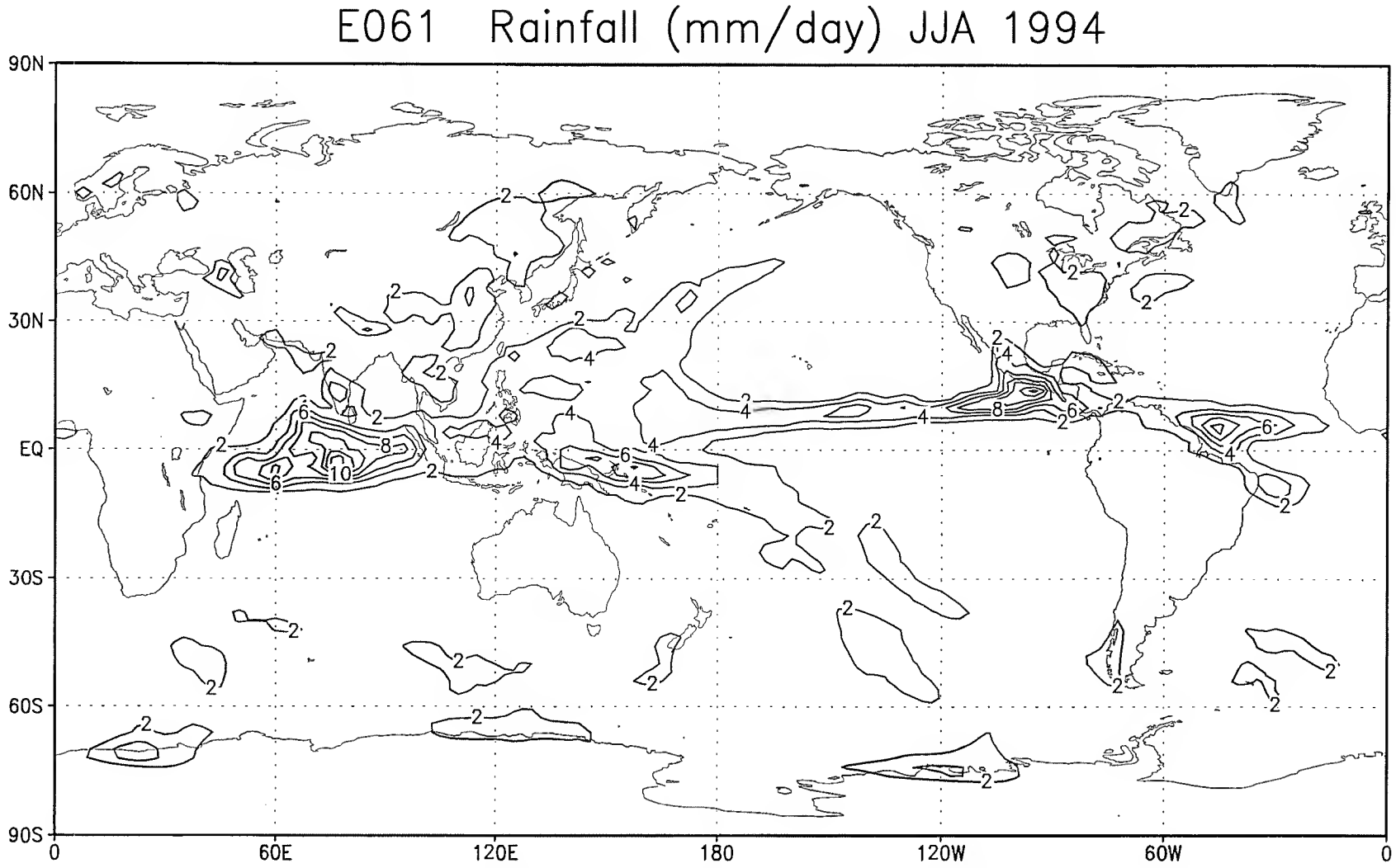

Fig. 5.b June-July-August mean precipitation (mm/day) in 1994 for FME2.

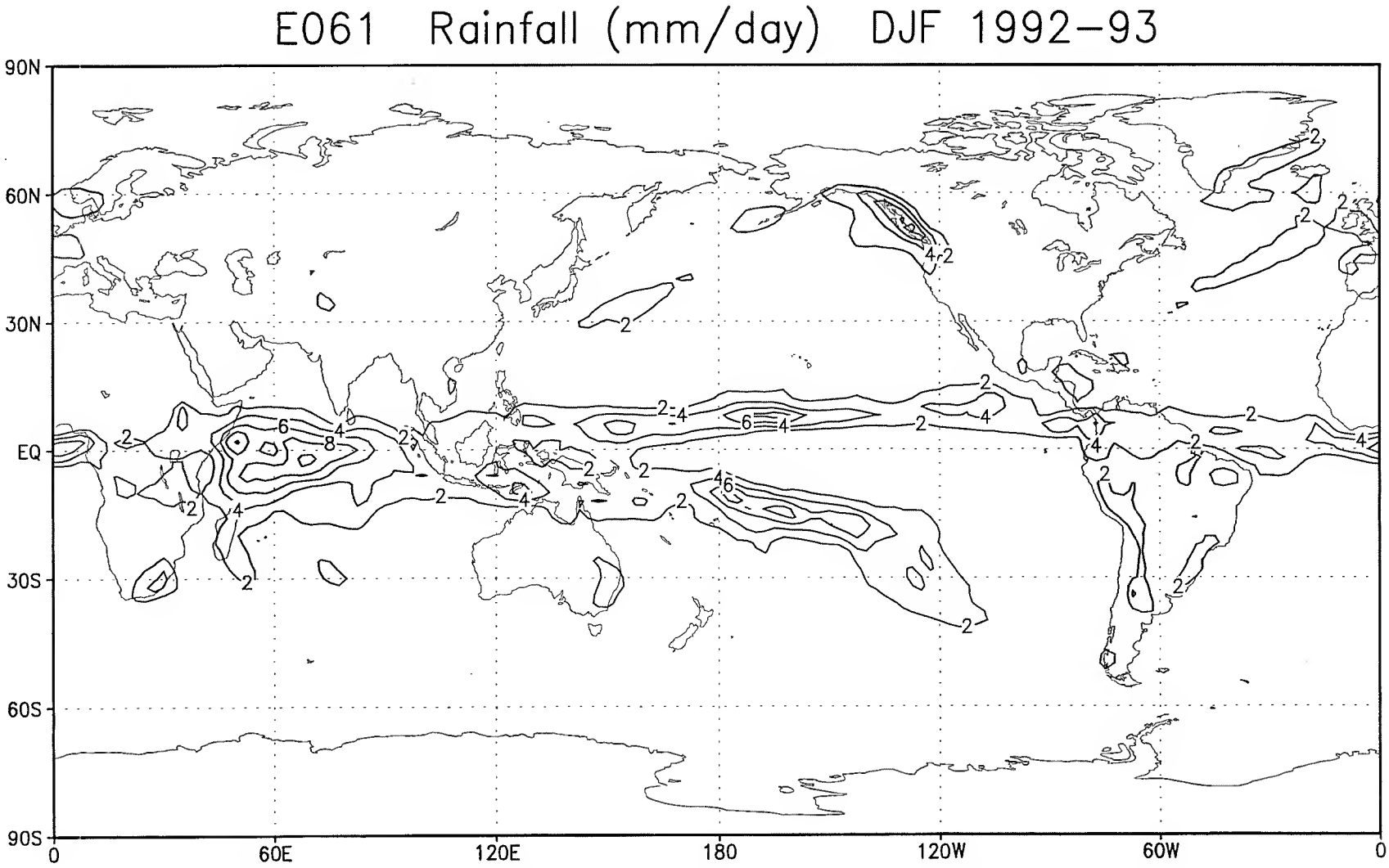

Fig. 5.c December-January-February mean precipitation (mm/day) in 1992-93 for FME2.

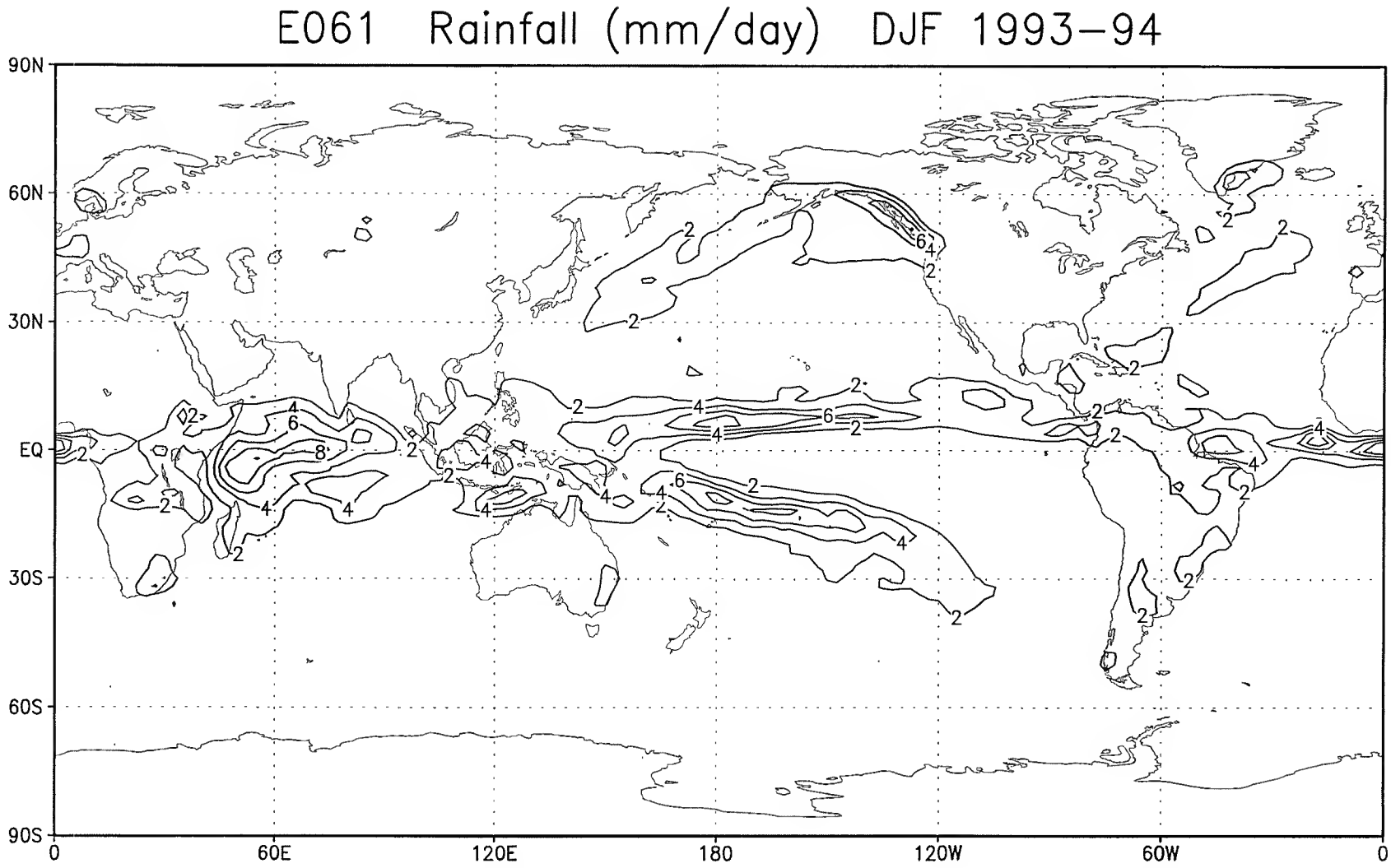

Fig. 5.d December-January-February mean precipitation (mm/day) in 1993-94 for FME2.

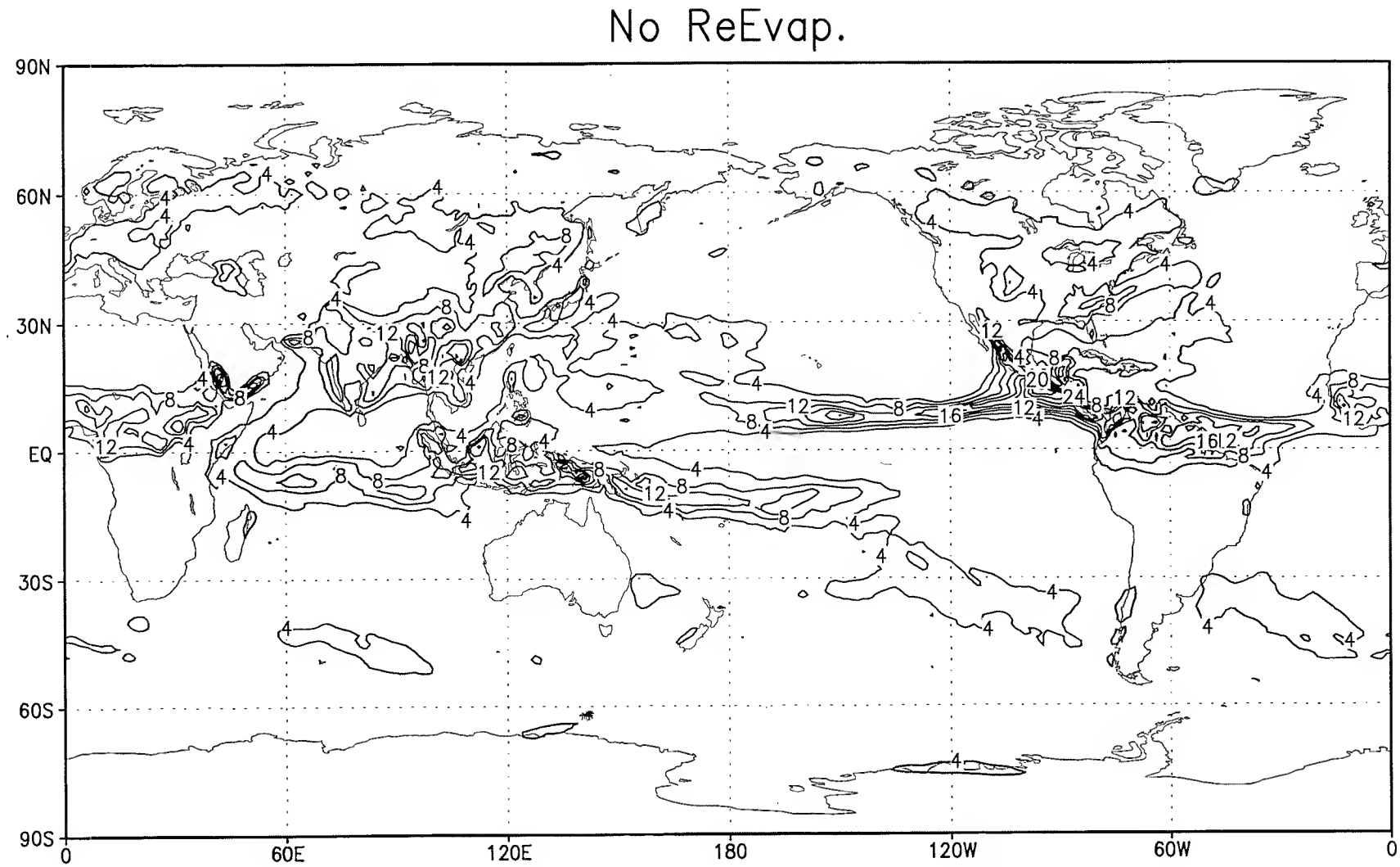

Fig. 6a June-July-August mean precipitation (mm/day) in 1995 without rain re-evaporation in an experiment with horizontal resolution doubled.

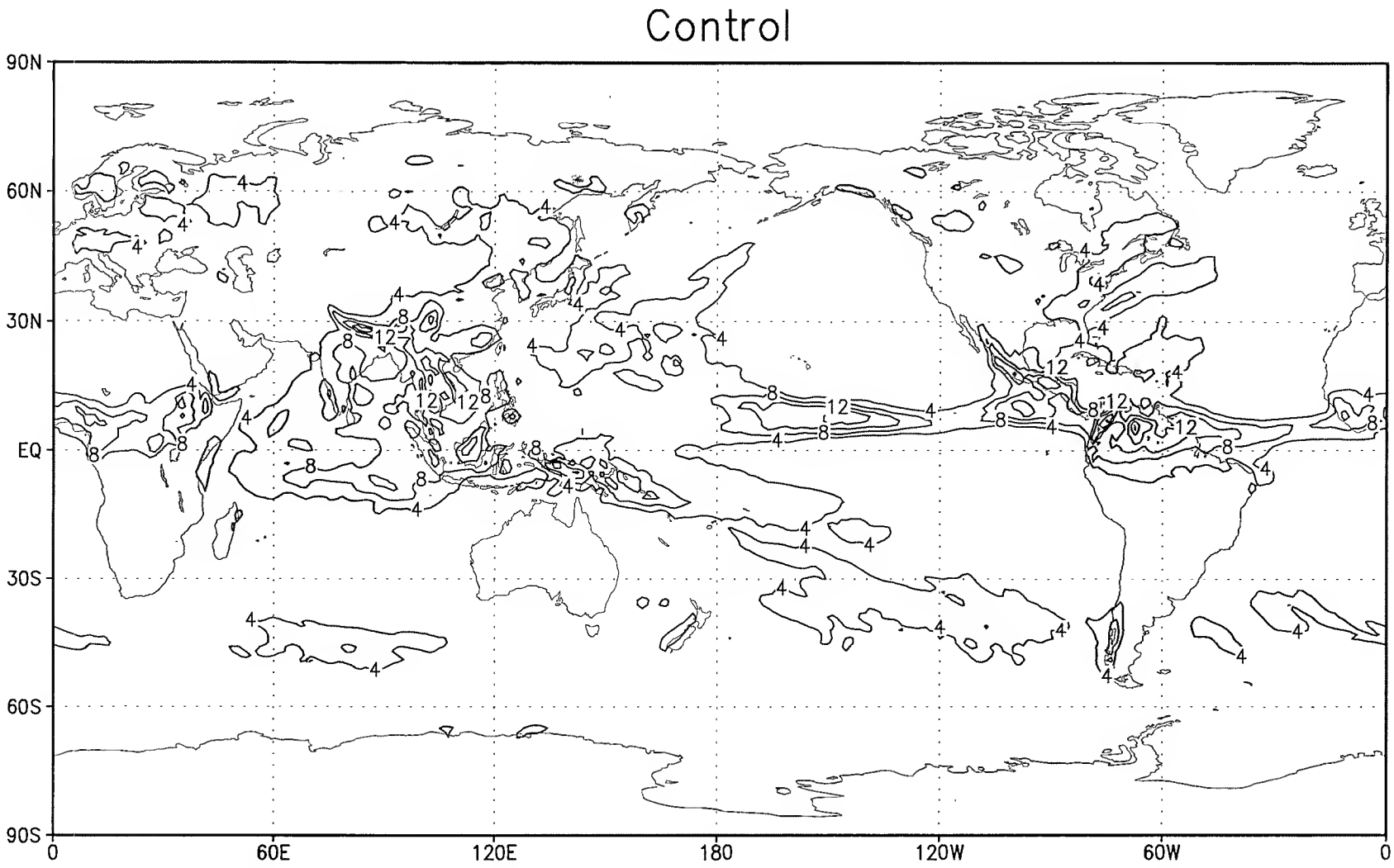

Fig. 6b June-July-August mean precipitation (mm/day) in 1995 with rain re-evaporation in an experiment with horizontal resolution doubled.

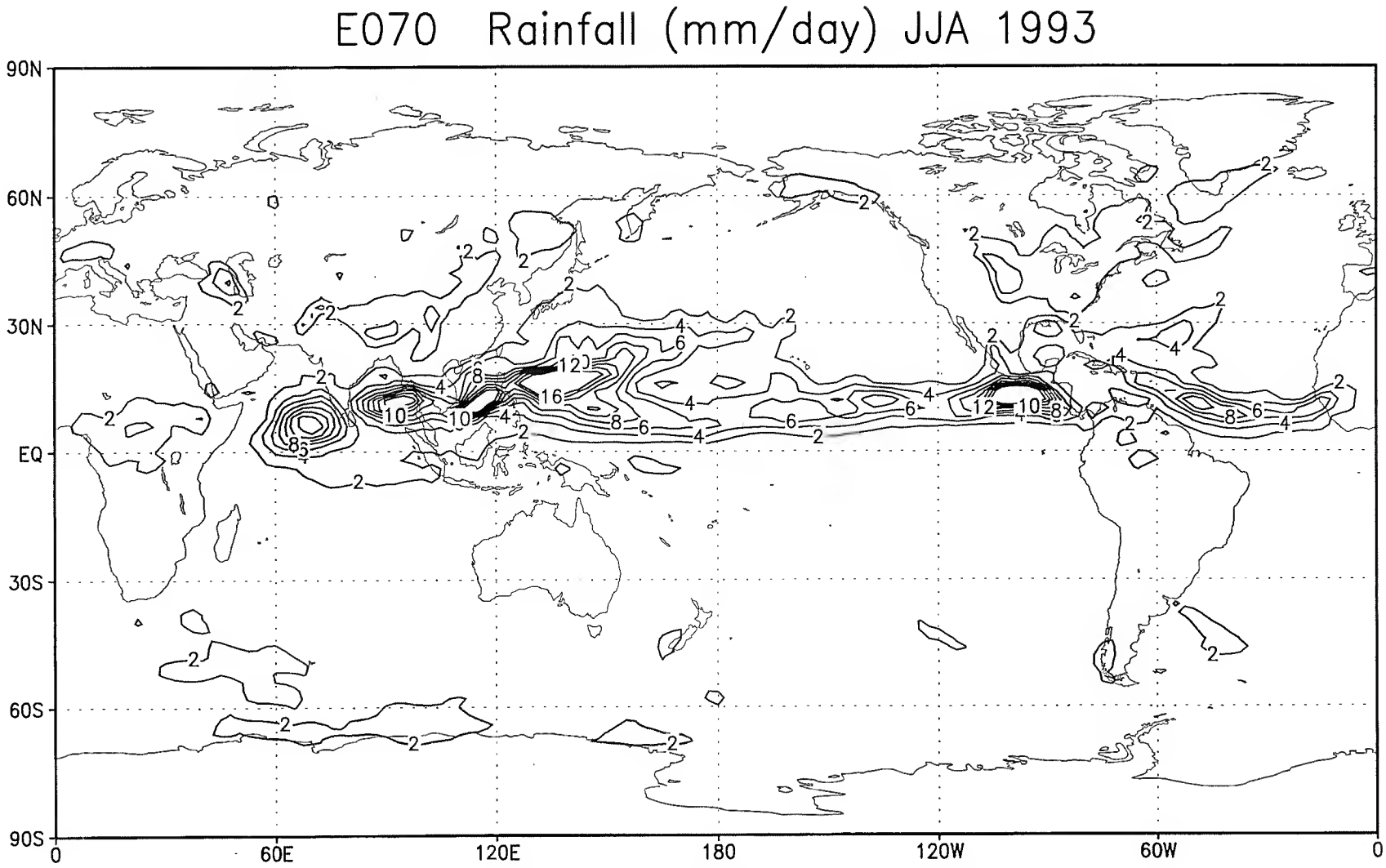

Fig. 7 June-July-August mean precipitation (mm/day) in 1993 for FME3.

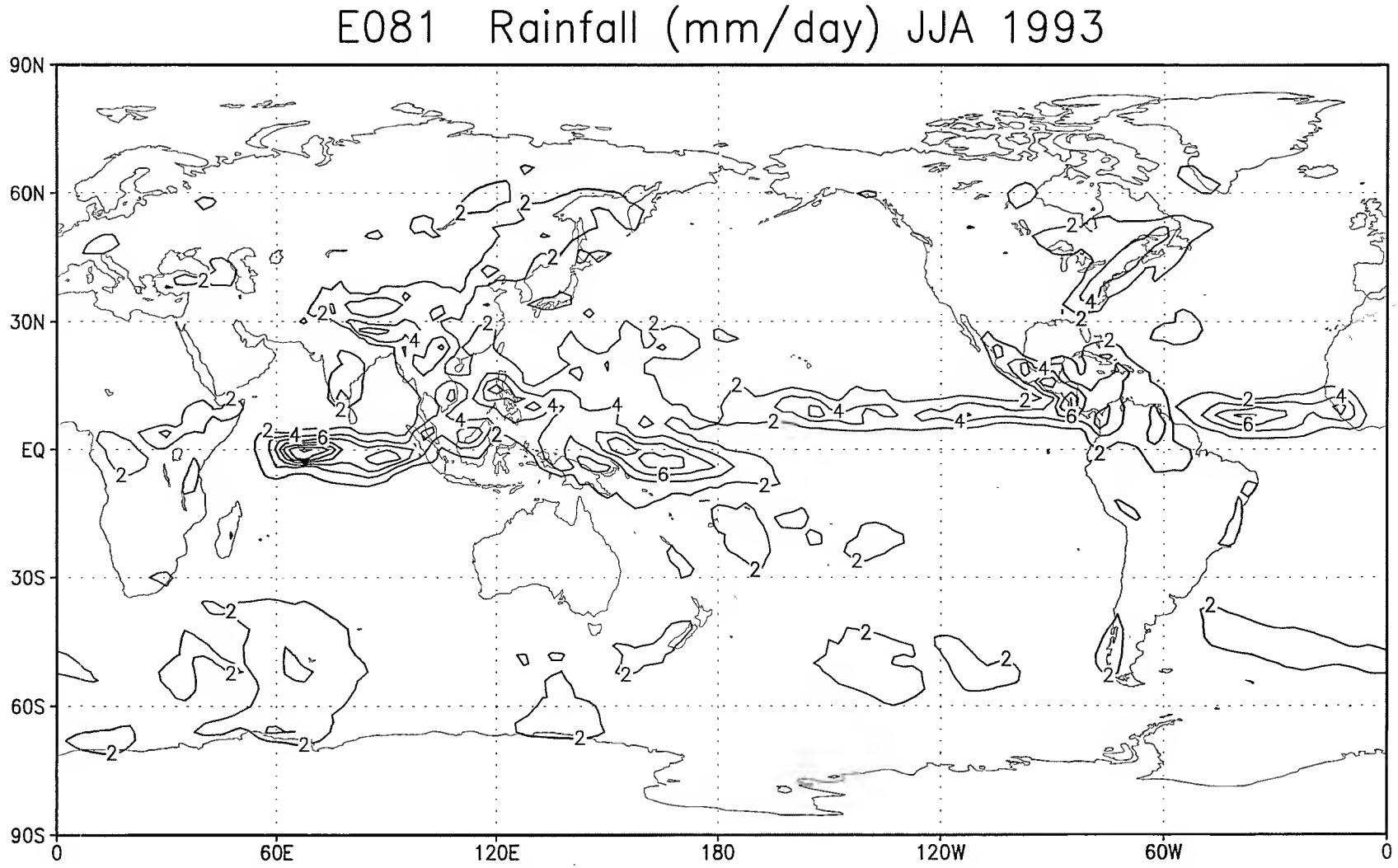

Fig. 8 June-July-August mean precipitation (mm/day) in 1993 for FME4.